biomedicines

MDPI

Article

Exploratory Untargeted Serum Lipidomics Identifies Altered Phospholipid and Glycerolipid Features in Established Type 2 Diabetes Mellitus

Jumana Y. Al-Aama [1,2], Hadiah B. Al Mahdi [3,4], Rawabi Zahed [3], Khadija Bakur [1,2], Amani Alhozali [4], Hala H. Mosli [4], Suhad Bahijri [5,6], Ahmed Bahieldin [3,7,8], Lothar Willmitzer [8], Abdulwahab S. Almutairi [9], Ashraf A. ElHarouni [1], Ola H. Elgaddar [10], Ahmed F. Bakry [11] and Sherif Edris [2,3,7,12,*]

[1] Department of Genetic Medicine, Faculty of Medicine, King Abdulaziz University, Jeddah 21859, Saudi Arabia
[2] Princess Al Jawhara Albrahim Centre of Excellence in Research of Hereditary Disorders, King Abdulaziz University, Jeddah 21589, Saudi Arabia
[3] Biological Sciences Department, Faculty of Science, King Abdulaziz University, Jeddah 21589, Saudi Arabia
[4] Department of Endocrinology and Metabolism, Faculty of Medicine, King Abdulaziz University, Jeddah 21589, Saudi Arabia
[5] Department of Clinical Biochemistry, Faculty of Medicine, King Abdulaziz University, Jeddah 21589, Saudi Arabia
[6] Saudi Diabetes Study Research Group, King Fahd Medical Research Center, King Abdulaziz University, Jeddah 21589, Saudi Arabia
[7] Centre of Excellence for Bionanoscience Research, King Abdulaziz University, Jeddah 21589, Saudi Arabia
[8] Max Planck Institute of Molecular Plant Physiology, Potsdam Science Park Am Muehlenberg, 14476 Potsdam, Germany
[9] The Ministry of Health, Jeddah 23344, Saudi Arabia
[10] Department of Chemical Pathology, Alexandria University, Alexandria 21526, Egypt
[11] Department of Molecular Biology, Al Borg Diagnostics, Jeddah 23226, Saudi Arabia
[12] Department of Genetics, Faculty of Agriculture, Ain Shams University, Cairo 11241, Egypt
* Correspondence: sedris@aucegypt.edu

Abstract

Background: Type 2 diabetes mellitus (T2DM) is associated with dysregulated lipid metabolism, but the serum lipid species associated with established T2DM may vary across populations and analytical platforms. We conducted an exploratory cross-sectional untargeted lipidomic analysis to characterize serum lipid features differing between adults with established T2DM and control participants. **Methods**: Serum samples from 36 patients with T2DM and 33 controls were analyzed by ultra-performance liquid chromatography-Orbitrap mass spectrometry. Lipidomic variation was assessed by principal component analysis and hierarchical clustering, followed by univariate analysis of putatively annotated lipid species, covariate-adjusted models, correlation with glycemic and lipid parameters in patients, and internally cross-validated receiver operating characteristic analysis. **Results**: Several phosphatidylcholine species (PC 38:4, PC 38:5, and PC 40:8) and PE 38:1 were higher in T2DM, whereas PI 36:1, TAG 54:6, and PC 32:2 were lower. These associations persisted after adjustment for age, sex, and body mass index and in participants with comparable reported fasting duration (>8 h but <10 h), but none of the principal species correlated significantly with HbA1c, plasma glucose, triglycerides, non-HDL cholesterol, or the triglyceride-glucose index among patients. A sex-by-disease interaction was supported only for PE 36:1, which was elevated predominantly in female patients. **Conclusions**: In this exploratory cross-sectional cohort, established T2DM was associated with selective differences in putatively annotated phospholipid and glycerolipid features. These findings do not establish causality,

Academic Editor: Arleta Drozd

Received: 12 September 2026
Revised: 15 October 2026
Accepted: 26 October 2026
Published: 28 October 2026

Copyright: © 2026 by the authors. Licensee MDPI, Basel, Switzerland. This article is an open access article distributed under the terms and conditions of the Creative Commons Attribution (CC BY) license.

specificity for diabetes relative to broader metabolic dysfunction, or diagnostic utility and require future confirmation in larger longitudinal cohorts with targeted quantification and independent validation.

Keywords: Type 2 diabetes mellitus; lipidomics; phosphatidylethanolamine; mass spectrometry; sex differences

1. Introduction

Type 2 diabetes mellitus (T2DM) is a complex, multifactorial metabolic disorder characterized by persistent hyperglycemia and impaired insulin signaling, and it continues to exert a significant global public health impact [1]. Although its etiopathogenesis remains incompletely elucidated, a growing body of evidence indicates that systemic perturbations in lipid and protein metabolism across multiple organ systems are central to both the initiation and progression of the disease [2]. A hallmark pathophysiological feature of T2DM is insulin resistance, defined as a diminished biological response of peripheral tissues, most notably skeletal muscle, to insulin-mediated glucose uptake [3]. This defect is strongly associated with obesity, particularly visceral (central) adiposity, giving rise to the construct of "diabesity," which underscores the interrelated nature of excess adiposity, neuroendocrine dysregulation, and metabolic dysfunction [4]. Beyond sedentary lifestyle and alterations in birth weight, functional derangements in key metabolic organs, including adipose tissue and the liver, are now recognized as major determinants of T2DM onset and progression [5].

Currently, the clinical diagnosis of T2DM relies predominantly on the detection of elevated blood glucose concentrations in conjunction with characteristic clinical manifestations. Standard diagnostic modalities include the oral glucose tolerance test and the measurement of glycated hemoglobin (HbA1c), with values of 39–47 mmol/mol (5.7–6.4%) indicating an increased risk of T2DM and values ≥48 mmol/mol (6.5%) meeting the diagnostic threshold for diabetes. Nevertheless, these conventional indices predominantly capture relatively advanced stages of metabolic dysregulation rather than the earliest molecular or physiological perturbations associated with disease onset. Although decreased high-density lipoprotein (HDL) cholesterol is widely employed as a lipid-related clinical parameter, there remains a notable paucity of biomarkers with sufficient sensitivity and specificity to reliably predict the early onset or progression of T2DM [6,7]. Accordingly, the discovery and validation of robust early-stage biomarkers continue to represent a major unmet need in clinical practice.

In response to this unmet clinical and translational need, increasing attention has been directed toward lipidomics as a promising and systematic strategy for biomarker discovery. In contrast to metabolomics, which broadly surveys low molecular-weight metabolites, lipidomics is dedicated to the comprehensive characterization of lipid species, encompassing their structural diversity, biochemical properties, and associated biological interaction networks [8]. Lipids function not only as fundamental structural constituents of cellular membranes but also as bioactive mediators that are indispensable for the regulation of energy homeostasis and the orchestration of intracellular and intercellular signal transduction processes [9]. Individuals with insulin resistance frequently display a characteristic dyslipidemic profile, involving both quantitative and qualitative perturbations in circulating lipid species [10]. Several lipid classes, including fatty acids, acylglycerols, and ceramides, have been mechanistically implicated in the pathogenesis of T2DM [11]. Among these, ceramide metabolism has emerged as a particularly compelling therapeutic target, while specific lipidomic signatures are

increasingly being evaluated as candidate biomarkers for susceptibility to insulin resistance and related metabolic dysfunction [12].

Prospective longitudinal investigations have evaluated the prognostic utility of circulating lipid biomarkers. In particular, higher triglyceride concentrations and dysregulated low-density lipoprotein/high-density lipoprotein (LDL/HDL) ratios have been associated with an increased subsequent risk of developing impaired fasting glucose [13]. In addition, metabolomics-based investigations indicate that distinct lipid signatures may predict progressive decline in pancreatic islet β-cell function and the transition from early metabolic dysregulation to clinically manifest T2DM [14,15]. However, the identification of universally applicable lipid biomarkers remains challenging, as lipid metabolism is intrinsically dynamic and is profoundly modulated by dietary, environmental, and genetic factors. Recent advances in mass spectrometry (MS)-based analytical platforms, including direct infusion and liquid chromatography-mass spectrometry (LC-MS), have substantially improved the sensitivity, selectivity, and reproducibility of lipidomic profiling [16]. When coupled with bioinformatics and systems biology methodologies, these high-throughput technologies facilitate comprehensive characterization of lipid species diversity and their covalent modifications, thereby providing more nuanced insights into disease-associated metabolic reprogramming [17,18]. Nevertheless, a large proportion of the current evidence is derived from cross-sectional investigations, which constrains the ability to infer the temporal dynamics and mechanistic underpinnings of lipid dysregulation during the progression of T2DM. In this context, the present exploratory study aimed to characterize serum lipid features that differ between adults with established T2DM and control participants using untargeted UPLC-Orbitrap lipidomics and to examine how the principal features relate to the clinical and metabolic characteristics of the participants.

2. Materials and Methods

2.1. Study Design and Participants

This case–control study included 36 patients with clinically confirmed T2DM and 33 control participants; all participants were recruited from the Endocrinology Clinics at King Abdulaziz University Hospital (KAUH), Jeddah, Saudi Arabia. The T2DM group comprised 10 males and 26 females, whereas the control group comprised 10 males and 23 females; Saudi nationals formed the largest group (33 of 69 participants, 47.8%; Figure S1). Exclusion criteria included clinically documented advanced liver failure or end-stage liver disease and clinically documented end-stage renal disease or dialysis-dependent renal failure, as recorded in their medical history. Demographic, clinical, and anthropometric data were collected, including age, sex, height and weight (from which body mass index [BMI] was calculated), blood pressure, heart rate, medical history (including diabetes duration where documented), current pharmacotherapy, smoking status, and, for participants with T2DM, lifestyle characteristics (Table S1). Routine laboratory assessments, which were available for participants with T2DM (Table S1), included hemoglobin concentration, glycated HbA1c, plasma glucose (measured in fluoride/oxalate plasma obtained at the same venipuncture as the serum samples used for lipidomic analysis), serum creatinine, thyroid-stimulating hormone, low-density lipoprotein cholesterol (LDL-C), high-density lipoprotein cholesterol (HDL-C), total cholesterol, and triglycerides. The diagnosis of T2DM was established according to the American Diabetes Association (ADA) criteria in effect at the time of enrollment: fasting plasma glucose ≥126 mg/dL, 2-h plasma glucose ≥200 mg/dL during a standard oral glucose tolerance test, or HbA1c ≥ 6.5% (48 mmol/mol) [19]. Control participants were recruited from individuals without a prior diagnosis of diabetes or other documented

metabolic disease and who were not receiving glucose-lowering therapy at the time of enrollment.

2.2. Ethical Approval

The study protocol was reviewed and approved by the Unit of Biomedical Ethics, Faculty of Medicine, King Abdulaziz University, Jeddah, Saudi Arabia (Reference No. IEE-20; approved on 1 October 2018). All procedures were conducted in accordance with the ethical principles of the Declaration of Helsinki, and written informed consent was obtained from all participants prior to their enrollment in the study.

2.3. Blood Collection and Sample Preparation

To reduce circadian-associated variability, venous blood samples were obtained in the morning (08:00–10:30 h). Fasting duration was obtained by participant self-report; all participants reported an overnight fast of >8 h. The case report form recorded fasting duration as a binary item (fasted ≥10 h: yes/no), so that 'Yes' indicated a reported fasting duration of ≥10 h and 'No' a reported duration of >8 h but <10 h; fasting duration was not independently measured by the study team, and exact fasting times were not recorded. Accordingly, 23 of 36 participants with T2DM and 1 of 33 control participants were classified as reporting fasting ≥10 h, whereas 13 participants with T2DM and 32 control participants were classified as reporting fasting >8 h but <10 h (Table S1). Blood was drawn into serum gel tubes, gently inverted twice, and allowed to clot for 30 min at ambient temperature (25 °C). Subsequently, samples were centrifuged at 2750× *g* for 10 min at 15 °C. The resulting serum was aliquoted, maintained at 4 °C for a maximum of 6 h, and then stored at −80 °C until analysis, whereas repeated freeze–thaw cycles were rigorously avoided. For lipid extraction, serum aliquots were combined with a pre-chilled (−20 °C) monophasic solvent mixture composed of methanol, methyl tert-butyl ether (MTBE), and water (1:3:1, v/v/v). The use of a pre-chilled monophasic MTBE-based system enables the concurrent extraction of lipids and polar metabolites. Samples were agitated on an orbital shaker for 30 min at 4 °C and subsequently subjected to ultrasonication in an ice-cooled ultrasonic bath for 10 min to enhance extraction efficiency. Thereafter, a methanol:water solution (1:3, v/v) was added to induce biphasic phase separation. Following vortex mixing and centrifugation, the upper organic phase containing lipids and the lower aqueous phase containing polar and semi-polar metabolites were collected separately, vacuum-dried, and stored at −80 °C until further analysis. All serum specimens were collected and processed using the same standardized pre-analytical workflow to minimize between-group technical variation.

2.4. Lipidomic Analysis

Lipidomic profiling was performed using a Waters ACQUITY Ultra-Performance Liquid Chromatography (UPLC) system coupled to an Exactive Orbitrap mass spectrometer (Thermo Fisher Scientific, Waltham, MA, USA). Dried lipid extracts were reconstituted in 500 µL acetonitrile:isopropanol (7:3, v/v), and 2 µL of each reconstituted sample was injected for analysis. Chromatographic separation was conducted on a reversed-phase C8 column (100 mm × 2.1 mm, 1.7 µm; Waters) maintained at 55 °C. The mobile phase consisted of buffer A (water containing 10 mM ammonium acetate and 0.1% acetic acid) and buffer B (acetonitrile:isopropanol, 7:3, v/v, containing 10 mM ammonium acetate and 0.1% acetic acid). Ammonium acetate was supplied as a 1 M stock solution and added at 1% (v/v) to obtain a working concentration of 10 mM. Separation was carried out at a flow rate of 400 µL/min using a multistep gradient elution over a total analysis time of 22 min.

Mass spectrometric data were acquired in full-scan and all-ion fragmentation (AIF) modes over an m/z range of 100–1500. The Orbitrap mass analyzer was operated at a resolving power of 10,000, with a scan rate of 10 spectra/s and a maximum ion injection time of 100 ms. The heated electrospray ionization source was operated with a spray voltage of 3 kV and a capillary temperature of 150 °C. Data were acquired in both positive and negative ionization modes to maximize coverage of the lipidome, in accordance with established untargeted lipidomics workflows on Orbitrap-based platforms [20]. To ensure analytical robustness and reproducibility, pooled quality-control samples were generated by combining equal aliquots from all study samples and were injected at the beginning of the analytical sequence as well as at regular intervals throughout the run. Solvent blanks were interspersed to monitor background signal and potential carryover, and the injection order of study samples was randomized to minimize batch-related bias. No class-specific internal standards were incorporated into the present untargeted workflow. Consequently, the dataset is suitable for relative comparisons between experimental groups rather than for absolute quantification across lipid classes. Lipid features were putatively annotated based on accurate mass measurements, chromatographic retention times, and comparison with an in-house spectral library, following accurate-mass and fragmentation assisted annotation strategies routinely employed in LC-MS-based lipidomics. For the 93 annotated features, the measured m/z values agreed with the theoretical m/z of the assigned $[M+H]^+$ (PC and PE) or $[M+NH4]^+$ (PI and TAG) ions within ±6 ppm (range −5.9 to +5.4 ppm; median −2.4 ppm), and retention times deviated from the corresponding library entries by −0.03 to +0.30 min (Table S4). Annotations are reported at the lipid species (sum-composition) level according to the LIPID MAPS shorthand notation [21]. Fatty acyl chains were not assigned to the annotated features, which therefore correspond to the species (sum-composition) level of the Lipidomics Standards Initiative reporting hierarchy rather than to molecular species. Where chromatographically distinct features shared the same sum composition, each was analyzed separately and is identified by its Peak ID and m/z (Tables S4 and S5).

2.5. Data Processing, Quality Control, and Statistical Analysis

Raw LC-MS features were initially filtered to remove low-intensity signals, putative background contaminants, and features with a signal-to-noise ratio <3; features were retained if they were detected in at least 80% of the samples of at least one of the four subgroups (female controls, male controls, female patients, and male patients), yielding 1191 features (Table S3). Of these, 93 features were putatively annotated as PC, PE, PI, or TAG species, of which 92 were included in the processed dataset used for all statistical analyses (Table S4); each of these 92 features was detected in at least 82.6% of all samples. Peak intensities were normalized sample-wise to correct for differences in overall signal intensity between samples (raw intensities in Table S3; normalized intensities in Table S4). Annotations were cross-checked against the measured m/z, adduct, and molecular formula of each feature. For each annotated feature, the coefficient of variation (CV% = SD/mean × 100) was calculated within each of the four subgroups (female controls, male controls, female patients, and male patients). Because these CVs were computed across biological samples, they reflect combined biological and analytical variability rather than analytical precision alone; they were therefore used descriptively, with a median CV > 50% across the four subgroups serving as a descriptive flag for features with comparatively high combined biological and analytical variability. For multivariate analyses, normalized intensities were log2-transformed to improve distributional symmetry and Pareto-scaled. Unsupervised principal component analysis (PCA) and hierarchical clustering analysis (HCA) were conducted on the 92 annotated features, with HCA based on Pearson correlation distance and average linkage, to characterize global

lipidomic differences between the T2DM and control groups. For univariate analysis, patients and controls were compared using two-tailed Welch's t-tests applied to the normalized (non-log-transformed) intensities of each of the 92 annotated features. Sex-associated differences were assessed in the same way by comparing all female with all male participants, pooled across disease status. To control multiple hypothesis testing, p-values were adjusted across the 92 features using the Benjamini–Hochberg false discovery rate (FDR) procedure, and FDR < 0.05 was considered significant. Lipid features with FDR < 0.05 for the T2DM-control comparison were designated as discriminatory lipids and ranked by FDR. Receiver operating characteristic (ROC) curve analysis was performed for the top discriminatory lipid species, and the area under the curve (AUC) was calculated to describe their discriminatory performance within this case–control sample.

Statistical analyses and figures were produced in Python 3.12 (SciPy, statsmodels, scikit-learn, and matplotlib). To address potential confounding, each principal discriminatory feature (log2-transformed) was modeled by linear regression with disease status as the exposure and age, sex, and BMI as covariates; a disease status × sex interaction term was added to test formally whether disease-associated differences differed between women and men. Associations between the principal lipid features and HbA1c, plasma glucose, triglycerides, HDL-C, non-HDL-C (total cholesterol minus HDL-C), and the triglyceride-glucose (TyG) index, calculated as ln[triglycerides (mg/dL) × plasma glucose (mg/dL)/2] [22], were examined within the T2DM group using Spearman correlation; plasma glucose and triglycerides were measured in the same blood collection as the lipidomic samples. Because reported fasting duration exceeded 8 h in all participants but was ≥10 h in only part of the cohort, the TyG index was not interpreted as having been derived under uniformly confirmed ≥10-h fasting. Within the T2DM group, lipid levels were also compared between users and non-users of statins, metformin, and insulin (Mann–Whitney U test). Benjamini–Hochberg correction was applied within each family of tests. For ROC analysis, 95% confidence intervals of the AUC were obtained from 2000 stratified bootstrap resamples. To estimate the optimism introduced by selecting and evaluating features in the same participants, the complete procedure (ranking all 92 features by Welch's t-test and selecting either the top-ranked feature or the top five features combined in an L2-penalized logistic regression model) was repeated within the training folds of 50 repetitions of stratified 5-fold cross-validation and evaluated in the held-out folds; an optimism-corrected AUC was additionally estimated using Harrell's bootstrap procedure (200 resamples). Finally, cross-validated AUCs of a logistic model containing age, sex, and BMI were compared with those of the same model extended by individual lipid features. To assess whether the principal between-group differences depended on the imbalance in reported fasting duration, the eight principal features were re-analysed in participants reporting fasting >8 h but <10 h (13 patients and 32 controls) using the same linear models, without and with adjustment for age, sex, and BMI (12 of the 13 patients had complete covariate data), and their AUCs were re-estimated with 2000 stratified bootstrap resamples. Because fasting ≥10 h was reported by only one control participant, fasting category could not be meaningfully separated from disease status by adding it as a covariate to full-cohort models; its association with lipid levels was therefore estimated within the T2DM group (≥10 h vs. >8 h but <10 h, adjusted for age, sex, and BMI). Benjamini–Hochberg correction was applied across the eight features within each sensitivity analysis.

3. Results

3.1. Cohort Characteristics

The final analytical cohort comprised 69 participants, including 36 individuals with T2DM and 33 control participants. The demographic and clinical characteristics of the

study population are presented in (Table 1), with further distributional details shown in (Figure S1) and participant-level descriptive data provided in (Table S1). Participants with T2DM were significantly older than control participants, with mean ages of 52.19 and 43.79 years, respectively ($p = 0.00153$). The T2DM group was also significantly shorter than the control group (mean height: 156.34 vs. 162.55 cm; $p = 0.01505$). By contrast, mean body weight did not differ significantly between groups (76.97 vs. 74.74 kg; $p = 0.65032$). Participants with T2DM also had a significantly higher mean BMI than control participants (31.44 vs. 28.04 kg/m^2; $p = 0.04610$); the mean BMI in the T2DM group was within the obese range, whereas that in the control group fell within the overweight range. Marked between-group differences were observed in blood pressure parameters, as individuals with T2DM exhibited a higher mean systolic blood pressure than controls (136.70 vs. 118.52 mmHg; $p = 0.00271$), corresponding to an absolute difference of 18.18 mmHg. In contrast, mean diastolic blood pressure was significantly lower in the T2DM group compared with controls (70.70 vs. 81.48 mmHg; $p = 0.00023$). Mean heart rate did not differ significantly between groups (78.44 vs. 77.12 beats/min; $p = 0.69442$). Overall, the T2DM group was characterized by older age, higher BMI, and higher systolic blood pressure relative to control participants, while body weight and heart rate were broadly comparable. In participants with T2DM, the mean HbA1c was 8.74 ± 1.72% (n = 30), mean plasma glucose was 9.42 ± 4.75 mmol/L (n = 32), mean triglycerides were 1.76 ± 0.89 mmol/L (n = 32), and the mean TyG index was 9.27 ± 0.55 (n = 31). These clinical chemistry measurements were obtained from the same blood draw as the lipidomic samples; all participants reported an overnight fast of >8 h, but reported fasting duration was not consistently ≥10 h. Also, thirteen patients (36.11%) were receiving statins, 17 (47.22%) metformin, and 17 (47.22%) insulin.

Table 1. Demographic and clinical characteristics of participants with T2DM and control participants.

Characteristic	T2DM	Control	p-Value
Age (years)	52.19 ± 11.68 (36)	43.79 ± 9.39 (33)	0.00153
Height (cm)	156.34 ± 10.80 (33)	162.55 ± 9.30 (33)	0.01505
Weight (kg)	76.97 ± 18.94 (32)	74.74 ± 20.61 (33)	0.65032
BMI (kg/m^2)	31.44 ± 7.18 (32)	28.04 ± 6.24 (33)	0.04610
Systolic BP (mmHg)	136.70 ± 24.92 (30)	118.52 ± 20.64 (33)	0.00271
Diastolic BP (mmHg)	70.70 ± 11.12 (30)	81.48 ± 10.63 (33)	0.00023
Heart rate (bpm)	78.44 ± 13.99 (25)	77.12 ± 10.41 (33)	0.69442

Values are mean ± SD (n with available data); p-values are from Welch's two-sample t-test.

3.2. Feature-Level Variability (Coefficient of Variation)

For each of the 92 annotated features, the coefficient of variation (CV%) was computed within four predefined subgroups female controls, male controls, female patients, and male patients (Table S2). Because CVs were derived across individual participants, they describe biological-sample variability and incorporate both inter-individual biological heterogeneity and analytical variation; they should not be interpreted as direct estimates of analytical measurement reliability or analytical precision alone. Subgroup-specific CVs were therefore reported for descriptive purposes only, with a median CV > 50% used as an indicator of comparatively high overall variability rather than as an independent metric of analytical imprecision. The subgroup-specific median CVs were 42.42% for female controls, 41.84% for male controls, 39.30% for female patients, and 38.49% for male patients. Using a median CV threshold of 50% across the four subgroups as an indicator of greater biological-sample variability, 69 of 92 features

(75.00%) exhibited a median CV ≤ 50%, whereas 23 features (25.00%) exceeded this threshold; however, these features were retained for downstream analyses. At the lipid-class level, all phosphatidylinositol species displayed a median CV ≤ 50%, followed by phosphatidylcholine (88.9%) and phosphatidylethanolamine species (87.5%); in contrast, only 46.9% of triacylglyceride species met this criterion. Among the principal discriminatory features, median CVs were ≤50% for PI 36:1 (25.1%), PC 32:2 (38.8%), PC 40:8 (26.2%), PE 38:1 (31.0%), PC 38:4 (16.0%), and PC 38:5 (27.1%), whereas TAG 54:6 (51.2%) and TAG 48:4 (96.3%) exceeded 50% (Table S5). For TAG 54:6, CVs were comparatively low in controls (37.9% in female controls; 19.2% in male controls) but elevated in patients (64.6% and 75.4%, respectively), consistent with increased inter-individual heterogeneity in the patient group.

3.3. Global Lipidomic Profiles of T2DM and Control Participants

Multivariate analyses revealed a partial differentiation between participants with T2DM and control participants based on their serum lipidomic profiles (Figure 1). In the PCA score plot (Figure 1a), the first two principal components explained 20.6% and 16.6% of the total variance, respectively. Group discrimination by disease status was observed primarily along PC2, with T2DM samples predominantly exhibiting negative PC2 scores and control samples positive PC2 scores; by contrast, PC1 largely captured within-group heterogeneity. Despite this trend, substantial intergroup overlap persisted, with male participants in particular distributed across both disease categories. Hierarchical clustering (Figure 1b) resolved the cohort into two principal clusters: a T2DM-enriched cluster comprising 23 of 27 participants (85.2%) and a control-enriched cluster comprising 29 of 42 participants (69.0%). Collectively, these analyses indicate that the serum lipidome of individuals with T2DM differs from that of controls at a global level, although the incomplete separation shows that this difference is driven by a subset of lipid species rather than by a uniform shift.

At the lipid-class level (Figure 2), aggregated signal intensities showed substantial overlap across the four subgroups, with only minor shifts in central tendency (all ≤0.4 log2 units). For phosphatidylcholine (PC), total class intensity was modestly elevated in T2DM (mean log2 intensities: 30.05 in female controls, 30.00 in male controls, 30.22 in female patients, and 30.13 in male patients; FDR = 0.0038). Phosphatidylethanolamine (PE) exhibited a similarly modest increase in T2DM, driven predominantly by female patients (25.94 in female controls, 25.86 in male controls, 26.24 in female patients, and 25.89 in male patients; FDR = 0.0038). In contrast, phosphatidylinositol (PI; 23.96 in female controls, 23.81 in male controls, 23.90 in female patients, and 23.61 in male patients; FDR = 0.2687) and triacylglyceride (TAG; 31.39 in female controls, 31.76 in male controls, 31.53 in female patients, and 31.60 in male patients; FDR = 0.8844) did not differ significantly between T2DM and control groups. Collectively, these class-level results indicate that case–control differences were small when lipid classes were considered in aggregate, whereas greater discriminatory information was captured at the level of individual molecular species, including species exhibiting bidirectional changes within the same lipid class.

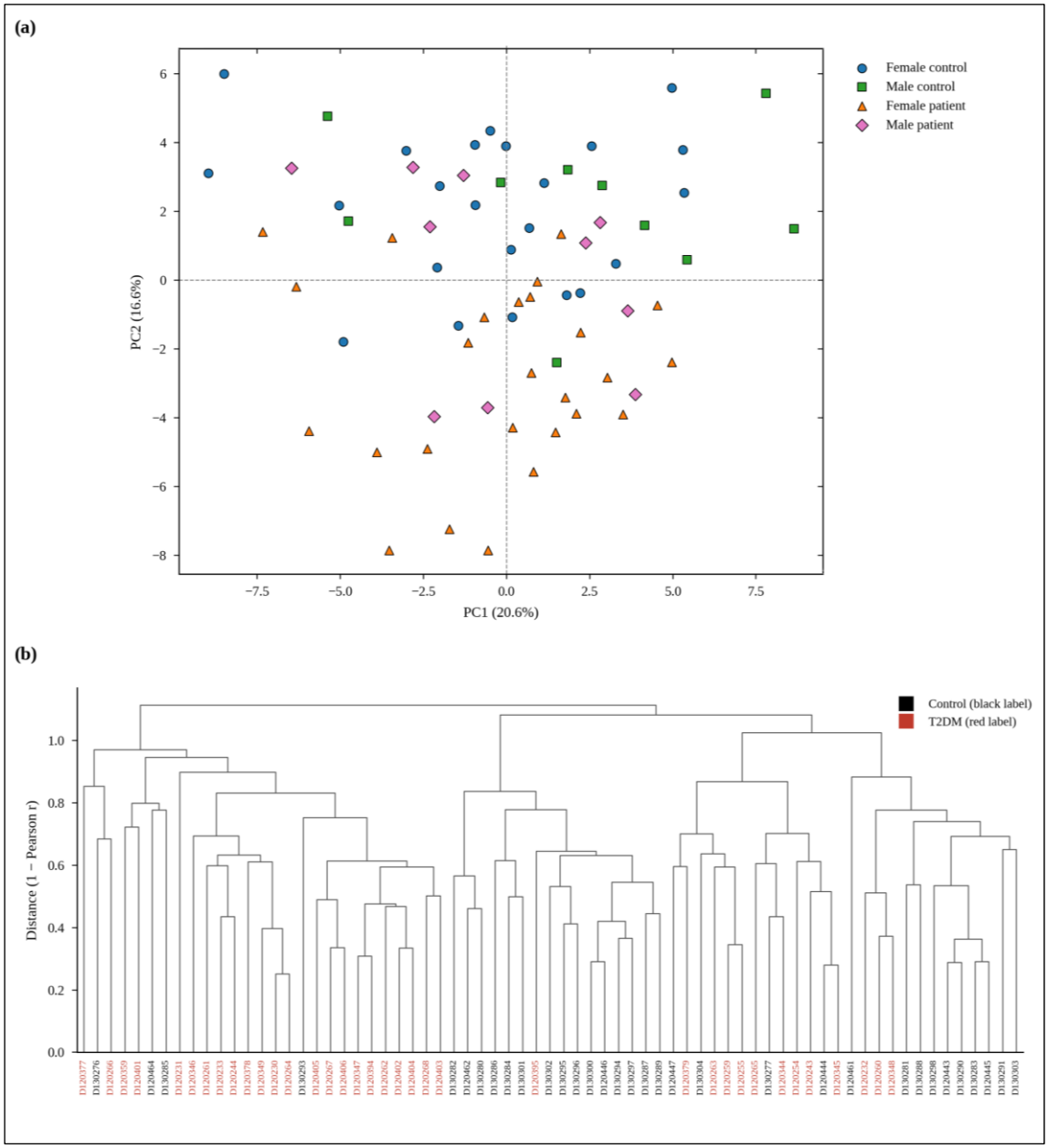


Figure 1. Multivariate analysis of global serum lipidomic profiles in control participants and patients with T2DM, based on the 92 annotated lipid features. (**a**) PCA score plot showing sample distribution along PC1 and PC2. (**b**) HCA dendrogram (Pearson correlation distance, average linkage); black and red sample labels indicate controls and T2DM patients, respectively.

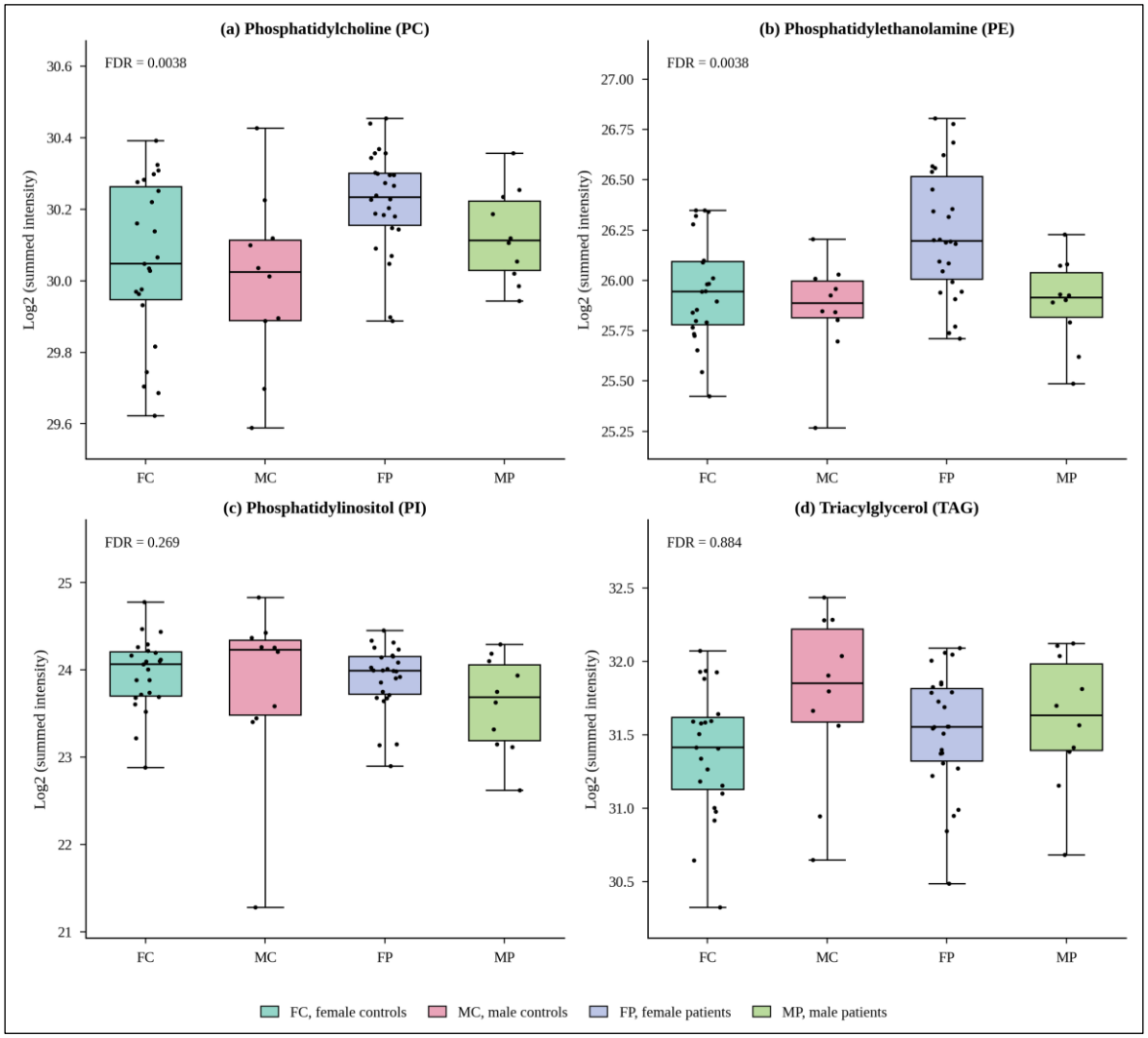


Figure 2. Distribution of aggregate lipid-class signals, normalized intensities of the putatively annotated features were summed on the linear scale within each class (PC, 36 features; PE, 16; PI, 8; TAG, 32) and log2-transformed for display: (**a**) phosphatidylcholine (PC), (**b**) phosphatidylethanolamine (PE), (**c**) phosphatidylinositol (PI), and (**d**) triacylglyceride (TAG), across female controls (FC), male controls (MC), female patients with T2DM (FP), and male patients with T2DM (MP). Dots represent individual participants, boxes indicate the interquartile range, and the central line indicates the median and whiskers show the range. FDR values refer to the T2DM versus control comparison (Welch's t-test, Benjamini–Hochberg correction across the four classes); main data are provided in Table S4.

3.4. PE Alterations in T2DM

Within the PE subclass, the quantified molecular species exhibited heterogeneous distributions across the four study subgroups, indicating that PE-related differences were contingent on the specific lipid species (Figure 3). PE 34:1 (Figure 3a) displayed higher levels in females than in males, with no detectable difference between T2DM and control groups (FDR = 0.4071), supporting a predominantly sex-associated pattern. In contrast, PE 36:1 (Figure 3b) was selectively increased in female participants with T2DM relative to the remaining three subgroups, whereas male patients did not differ from sex-matched controls; the overall patient–control contrast remained significant following FDR adjustment (FDR = 1.81×10^{-4}). PE 38:1 (Figure 3c) was elevated in both T2DM subgroups compared with both control subgroups (FDR = 4.87×10^{-6}). PE 38:5 (Figure 3d) exhibited substantial intergroup overlap and no significant case–control difference (FDR = 0.1942),

although a trend toward lower values was observed in male patients. Collectively, these results demonstrate species-specific PE alterations in T2DM: PE 38:1 was consistently increased in both sexes, PE 36:1 was increased primarily among female patients, and PE 34:1 and PE 38:5 varied by sex without evidence of a significant disease-associated effect.

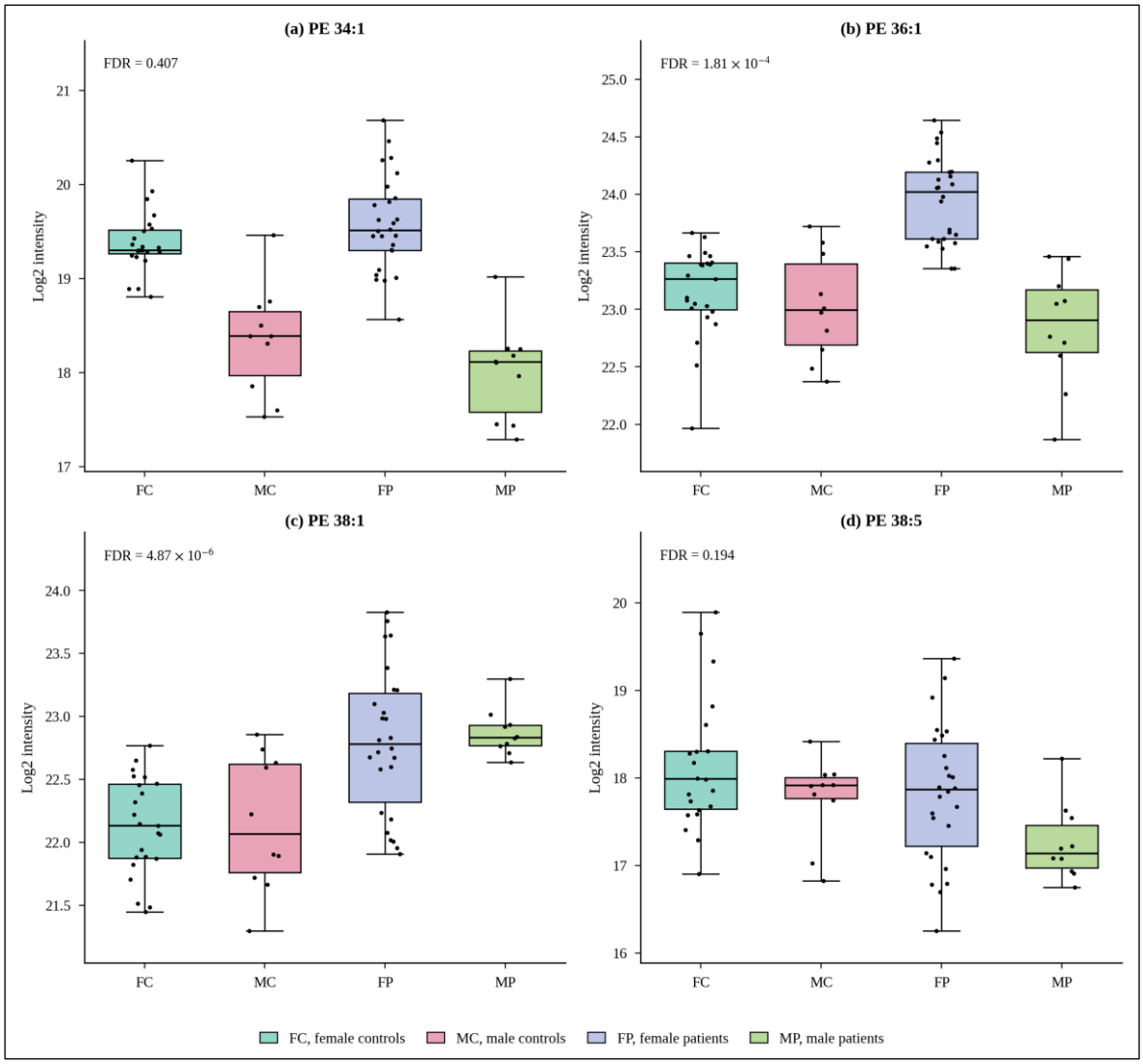


Figure 3. Comparison of serum phosphatidylethanolamine (PE) species across study groups. Panels (**a**–**d**) show PE 34:1 (Peak ID 2495), PE 36:1 (2646), PE 38:1 (2860), and PE 38:5 (2787), respectively. Data are presented for female controls (FC), male controls (MC), female patients with T2DM (FP), and male patients with T2DM (MP). Boxplots indicate the interquartile range and median, whiskers show the range, and dots represent individual participants. FDR values refer to the T2DM versus control comparison (Welch's t-test, Benjamini–Hochberg correction across 92 features); source data are provided in Table S4.

3.5. PC Alterations in T2DM

Among PC species, the four features with the lowest FDR values are presented in (Figure 4); three polyunsaturated PC species were increased in T2DM. Specifically, PC 38:4 (Figure 4b) exhibited an upward shift in both T2DM subgroups relative to both control subgroups, with the highest distribution observed in female patients (FDR = 4.81 × 10^{-6}). Conversely, PC 38:5 (Figure 4c) showed a concordant pattern, with both patient subgroups exceeding the corresponding control subgroups (FDR = 3.24 × 10^{-6}). Further, PC 40:8 (Figure 4d) was also elevated in both diabetic subgroups and provided the

strongest statistical evidence among the PC species (FDR = 1.39×10^{-7}). In contrast, PC 32:2 (Figure 4a) was decreased in T2DM, with the highest values observed in female controls and the lowest values in male patients (FDR = 5.24×10^{-6}). Collectively, these findings indicate bidirectional alterations in PC composition polyunsaturated species (PC 38:4, PC 38:5, and PC 40:8) were increased, whereas the less unsaturated PC 32:2 was decreased.

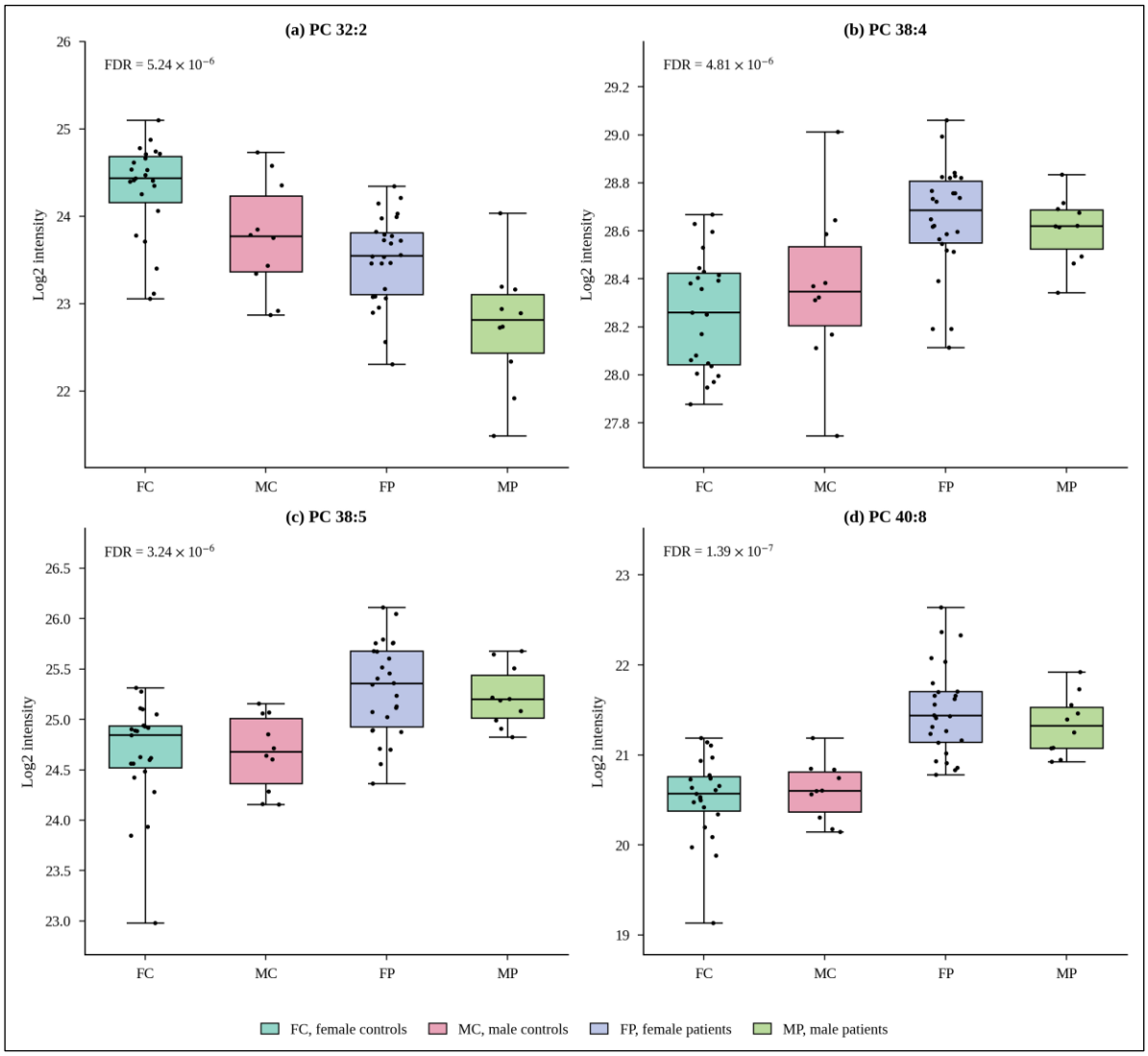


Figure 4. Comparison of serum phosphatidylcholine (PC) species across study groups. Panels (**a**–**d**) show PC 32:2 (Peak ID 2566), PC 38:4 (3286), PC 38:5 (3256), and PC 40:8 (3521), respectively. Data are presented for female controls (FC), male controls (MC), female patients with T2DM (FP), and male patients with T2DM (MP). Boxplots indicate the interquartile range and median, whiskers show the range, and dots represent individual participants. FDR values refer to the T2DM versus control comparison (Welch's t-test, Benjamini–Hochberg correction across 92 features); source data are provided in Table S4.

3.6. Reduced PI 36:1 in T2DM

Analysis of phosphatidylinositol (PI) 36:1 revealed a pronounced reduction in individuals with T2DM compared with control participants (Figure 5). In both sexes, control subgroups exhibited higher signal intensities than their respective T2DM counterparts, with female and male controls clustering at higher log2 intensity values, whereas female and male patients displayed a downward shift. This separation was consistently observed across sexes, suggesting a predominantly disease-associated effect

rather than a strongly sex-dependent influence. Although some intra-group variability was evident, particularly among female controls and female patients, the overall group distributions demonstrated minimal overlap, and the association remained highly significant after correction for multiple testing (FDR = 2.71×10^{-7}). Female and male patients showed similar distributions (median log2 intensity 18.27 and 18.15), both below those of female and male controls (19.10 and 19.06). Collectively, these results identify PI 36:1 as a robustly decreased phospholipid species in T2DM and support its contribution to the discriminatory lipidomic signature observed in this cohort.

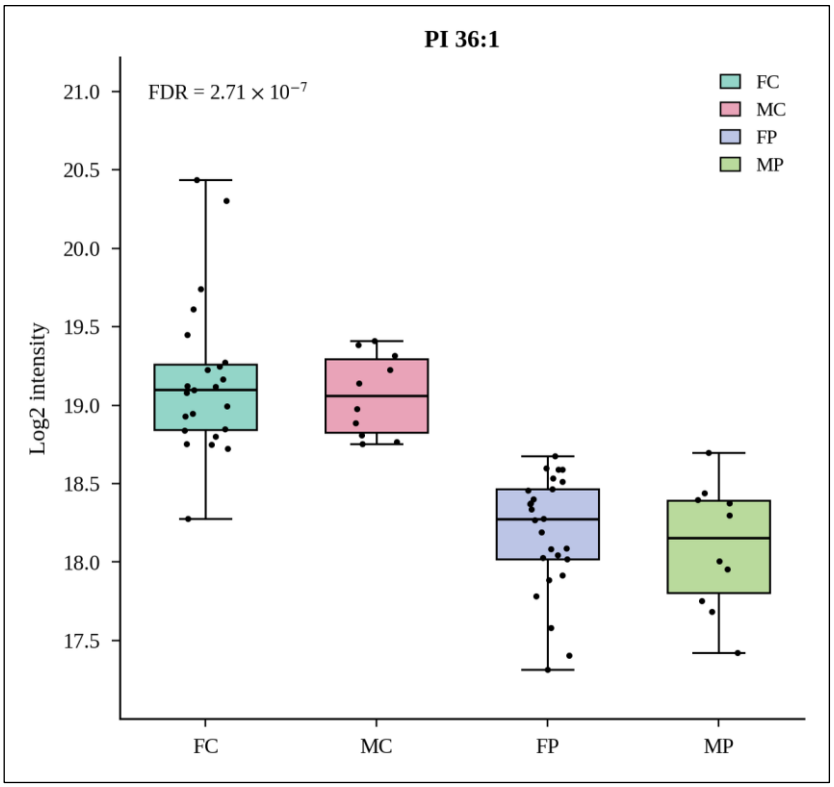


Figure 5. Comparison of serum phosphatidylinositol (PI) 36:1 across study groups. Data are presented for female controls (FC), male controls (MC), female patients with T2DM (FP), and male patients with T2DM (MP). Boxplots indicate the interquartile range and median, whiskers show the range, and dots represent individual participants, and the FDR value refers to the T2DM versus control comparison (Peak ID 4157; Welch's t-test, Benjamini–Hochberg correction across 92 features).

3.7. TAG Alterations in T2DM

The triacylglyceride (TAG) species shown in (Figure 6) displayed heterogeneous, species-specific responses rather than a uniform class-level shift. TAG 48:4 (Figure 6a) exhibited decreased signal intensities in both T2DM subgroups compared with the control subgroups, with the lowest levels observed in female patients (FDR = 0.0067). In contrast, TAG 52:4 (Figure 6b) and TAG 54:4 (Figure 6c) showed substantial overlap across the four subgroups and did not differ significantly between patients and controls (FDR = 0.3188 and 0.1823, respectively), although both species trended toward higher values in the male subgroups. The most prominent disease-associated difference was observed for TAG 54:6 (Figure 6d), which was shifted downward in both T2DM subgroups relative to both control subgroups (FDR = 2.58×10^{-11}), accompanied by increased dispersion among patients. Accordingly, within the TAG species evaluated, TAG 54:6 represented the most strongly reduced feature in T2DM, whereas TAG 48:4 showed a more modest decrease.

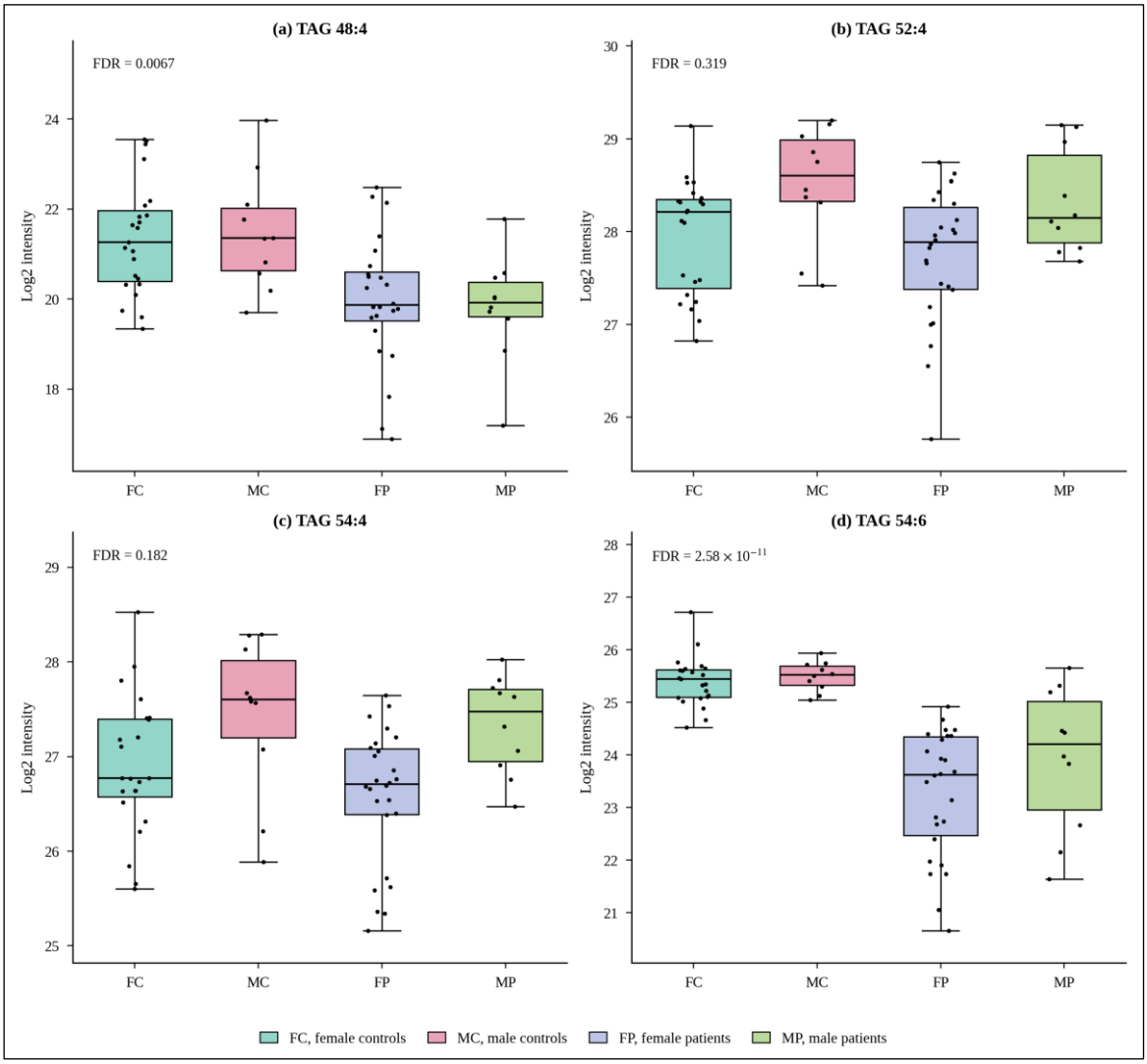


Figure 6. Comparison of serum triacylglyceride (TAG) species across study groups. Panels (**a**–**d**) show TAG 48:4 (Peak ID 3369), TAG 52:4 (4046), TAG 54:4 (4326), and TAG 54:6 (4284), respectively. Data are presented for female controls (FC), male controls (MC), female patients with T2DM (FP), and male patients with T2DM (MP). Boxplots indicate the interquartile range and median, whiskers show the range, and dots represent individual participants. FDR values refer to the T2DM versus control comparison (Welch's t-test, Benjamini–Hochberg correction across 92 features); source data are provided in Table S4.

3.8. Top Discriminatory Lipids Between Patients and Controls

Eight lipidomic features discriminating against individuals with T2DM from control participants displayed bidirectional changes (Figure 7). In total, 34 of 92 annotated features differed significantly between groups (FDR < 0.05; Table S5). The eight features highlighted correspond to the seven unique lipid species with the lowest FDR values, together with TAG 48:4, which was additionally selected as a second triacylglycerol (TAG) species despite ranking 15th; features ranked 8th–14th (including a second PC 38:4 feature, Peak ID 3285, PC 40:4, and PE 36:1) are reported in (Table S5). The upper panel depicts species reduced in T2DM: PI 36:1 (Figure 7a; FDR = 2.71 × 10^{-7}), PC 32:2 (Figure 7b; FDR = 5.24 × 10^{-6}), TAG 54:6 (Figure 7c; FDR = 2.58 × 10^{-11}; lowest FDR among all features), and TAG 48:4 (Figure 7d; FDR = 0.0067). For each of these lipids, both diabetic subgroups exhibited lower signal intensities than both control subgroups. The lower panel depicts species elevated in T2DM: PC 40:8 (Figure 7e; FDR = 1.39 × 10^{-7}), PE 38:1 (Figure 7f; FDR = 4.87 × 10^{-6}), PC 38:4 (Figure 7g; FDR = 4.81 × 10^{-6}), and PC 38:5 (Figure 7h; FDR = 3.24 ×

10^{-6}), with female patients generally showing the highest signal intensities. Overall, these results define a discriminatory lipid signature characterized by decreased PI 36:1, PC 32:2, and TAG abundance concomitant with increased polyunsaturated PC species and PE 38:1, consistent with selective remodeling of phospholipid and glycerolipid metabolism in T2DM.

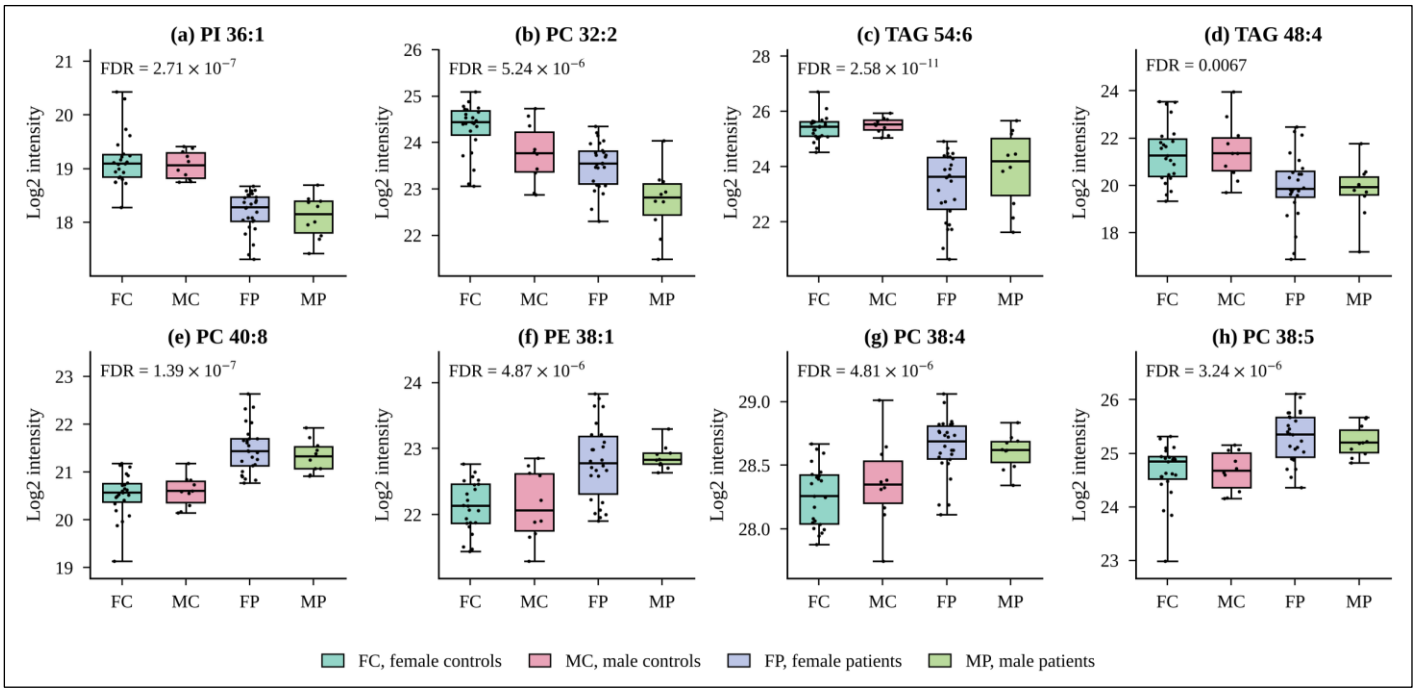


Figure 7. Eight discriminatory lipid features distinguish patients with T2DM from control participants. The upper row shows lipid species decreased in patients with T2DM: (**a**) PI 36:1 (Peak ID 4157), (**b**) PC 32:2 (2566), (**c**) TAG 54:6 (4284), and (**d**) TAG 48:4 (3369). The lower row shows lipid species increased in patients with T2DM: (**e**) PC 40:8 (3521), (**f**) PE 38:1 (2860), (**g**) PC 38:4 (3286), and (**h**) PC 38:5 (3256). Data are presented for female controls (FC), male controls (MC), female patients with T2DM (FP), and male patients with T2DM (MP). Boxplots indicate the interquartile range and median, whiskers show the range, and dots represent individual participants. FDR values refer to the T2DM versus control comparison (Welch's t-test, Benjamini–Hochberg correction across 92 features).

3.9. Sex-Associated Lipids

The lipid species with the strongest sex-associated differences are shown in (Figure 8); the FDR values in this figure compare all female with all male participants, pooled across disease status. PE 34:1 (Figure 8a) showed the strongest sex difference, with higher signal intensities in the female than in the male subgroups (FDR = 1.37×10^{-11}). PE 36:1 (Figure 8b) was also higher in women overall (FDR = 8.03×10^{-5}), but this difference arose almost entirely from female patients, who showed the highest signal intensities of all subgroups. A PC 38:5 feature (Peak ID 3257, chromatographically distinct from the disease-associated PC 38:5 feature in Figure 7h; Figure 8c) showed higher values in women (FDR = 0.0246). PE 38:5 (Figure 8d) was also higher in women, whereas TAG 54:4 (Figure 8e) and TAG 52:4 (Figure 8f) were higher in men (each FDR = 0.0316); PE 34:0 and PC 42:5, both higher in women, showed sex differences of similar magnitude (FDR = 0.0316; Table S5). Because these comparisons pool patients and controls, they describe sex differences rather than sex-specific disease effects. When a sex-by-disease interaction was formally tested in linear models adjusted for age and BMI (Table S5), a significant interaction was found only for PE 36:1 (interaction $\beta = -1.03$ log2 units, FDR = 3×10^{-4}),

reflecting an elevation confined largely to female patients. For PE 34:1, the sex difference was not significantly modified by disease status after correction (interaction $p = 0.036$, FDR = 0.25), and no interaction was detected for the eight principal discriminatory lipids (all FDR ≥ 0.89) or for the other sex-associated species; given that each male subgroup comprised only ten participants, these subgroup observations remain exploratory.

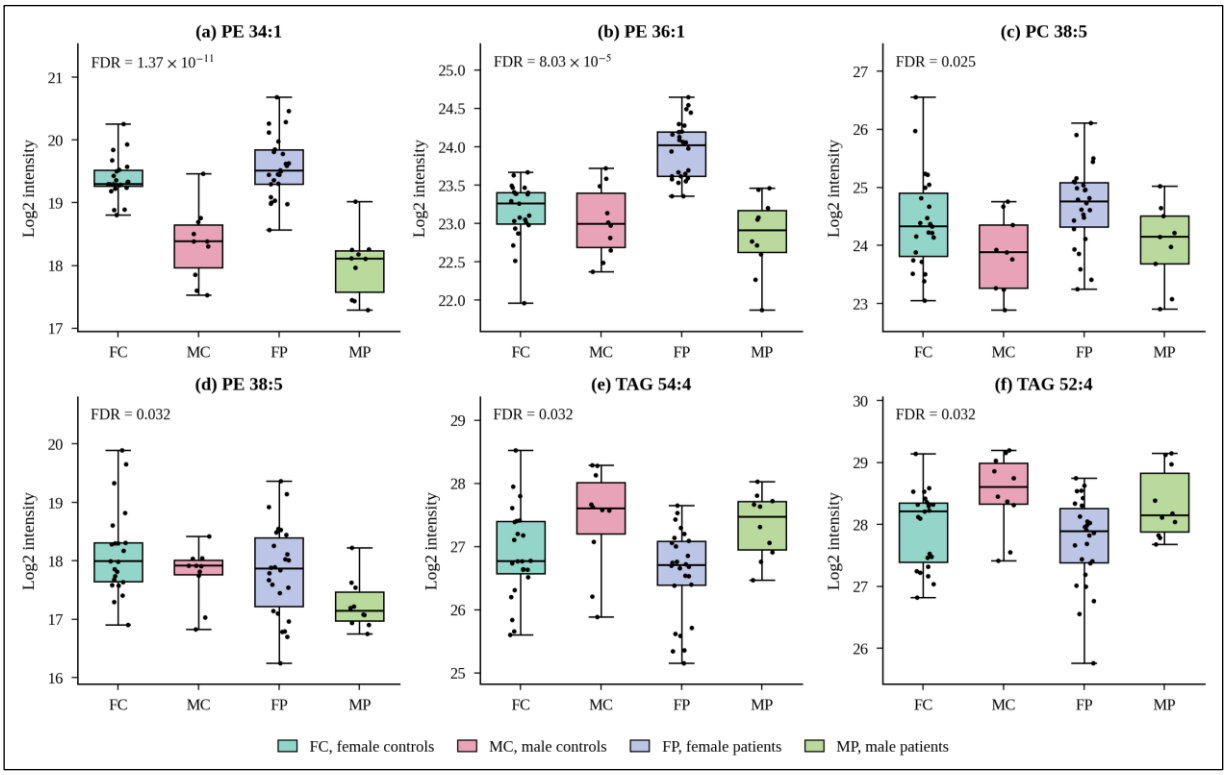


Figure 8. Sex-associated lipid features across study groups. Panels (**a**–**f**) show PE 34:1 (Peak ID 2495), PE 36:1 (2646), PC 38:5 (3257), PE 38:5 (2787), TAG 54:4 (4326), and TAG 52:4 (4046), respectively. Data are presented for female controls (FC), male controls (MC), female patients with T2DM (FP), and male patients with T2DM (MP). Boxplots indicate the interquartile range and median, whiskers show the range, and dots represent individual participants. FDR values refer to the comparison of all female with all male participants, pooled across disease status (Welch's t-test, Benjamini–Hochberg correction across 92 features).

3.10. Exploratory Discriminatory Performance of the Top Lipids

Receiver operating characteristic (ROC) curve analysis of the eight discriminatory lipid features (Figure 9) indicated that multiple lipid species differentiated individuals with T2DM from controls in this case–control dataset. PI 36:1 exhibited the highest discriminatory performance (AUC 0.985; 95% CI 0.949–1.000), followed by TAG 54:6 (AUC 0.955; 95% CI 0.894–0.995) and PC 40:8 (AUC 0.948; 95% CI 0.896–0.986). More modest discrimination was observed for PE 38:1 (AUC 0.867; 95% CI 0.770–0.939), PC 38:4 (AUC 0.851; 95% CI 0.755–0.932), PC 38:5 (AUC 0.840; 95% CI 0.737–0.918), PC 32:2 (AUC 0.822; 95% CI 0.717–0.918), and TAG 48:4 (AUC 0.795; 95% CI 0.689–0.891). Because feature selection and performance evaluation were conducted in the same participants, the resulting AUCs are likely upwardly biased due to overfitting. To quantify this bias, the full feature-selection pipeline was embedded within the training folds of 50 repetitions of 5-fold cross-validation; under this resampling framework, the top-ranked single feature (TAG 54:6; selected in 244 of 250 folds) achieved a mean held-out AUC of 0.954 (range 0.948–0.967 across repetitions), and the Harrell optimism-corrected AUC for the selected feature was 0.940 (estimated optimism 0.016). A baseline logistic regression model

including age, sex, and BMI yielded a cross-validated AUC of 0.67; addition of TAG 54:6 increased the AUC to 0.98, while inclusion of PI 36:1 and PC 40:8 increased the AUC to 0.97 and 0.92, respectively. Models incorporating multiple lipids approached complete separation (Table S5). The reported AUC values quantify discriminative performance within the present case–control cohort. However, reported fasting duration differed markedly between groups: 23/36 participants with T2DM, compared with 1/33 controls, reported fasting ≥10 h, whereas 13/36 participants with T2DM, compared with 32/33 controls, reported fasting >8 h but <10 h. Internal cross-validation can mitigate optimism arising from model fitting and feature selection but cannot correct for such between-group imbalances in sampling conditions; ROC performance was therefore re-estimated in participants reporting fasting >8 h but <10 h, in whom AUCs were similar to those in the full cohort (0.808–0.983 vs. 0.795–0.985) but had wider confidence intervals.

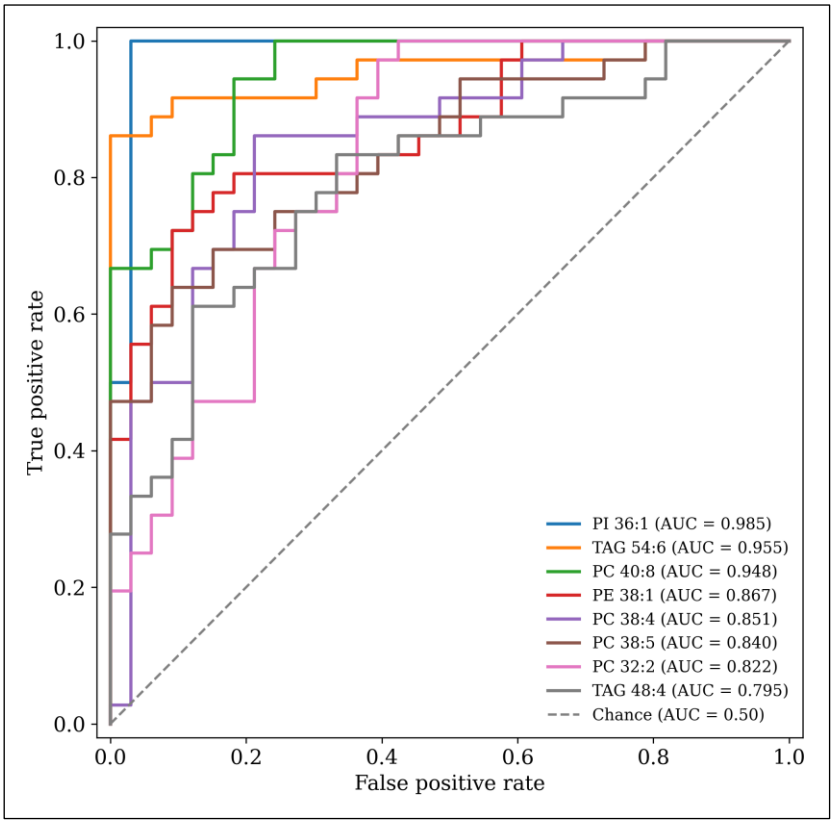


Figure 9. ROC curves for the eight discriminatory lipid features distinguishing patients with T2DM from control participants (log2 normalized intensities from Table S4). Curves are shown for PI 36:1, TAG 54:6, PC 40:8, PE 38:1, PC 38:4, PC 38:5, PC 32:2, and TAG 48:4, with their apparent AUC values; bootstrap 95% confidence intervals and cross-validated estimates are given in (Table S5). The dashed diagonal line represents chance-level classification (AUC = 0.50).

3.11. Adjustment for Clinical Covariates and Relation to Metabolic Parameters

After adjustment for age, sex, and BMI, all eight principal discriminatory features remained significantly associated with T2DM (all FDR ≤ 7×10^{-4}), and the effect sizes were comparable to those observed in unadjusted analyses (Table S5). For instance, TAG 54:6 was 2.17 log2 units lower (95% CI −2.61 to −1.72) and PI 36:1 was 0.93 log2 units lower (95% CI −1.15 to −0.72) in patients relative to controls. Within the T2DM cohort, none of the principal features exhibited significant correlations with HbA1c, plasma glucose, triglycerides, HDL-C, non-HDL-C, the TyG index, BMI, or age following FDR correction (all FDR > 0.5). Notably, TAG 54:6 was not associated with conventional serum triglycerides ($\varrho = 0.22$, $p = 0.23$) or the TyG index ($\varrho = 0.07$, $p = 0.69$). The largest nominal

associations were observed between PC 32:2 and the TyG index (ϱ = 0.41, p = 0.021) and between PI 36:1 and non-HDL-C (ϱ = −0.41, p = 0.037). After FDR adjustment, no lipid species differed significantly between users and non-users of statins, metformin, or insulin (all FDR ≥ 0.35). Diabetes duration was available for only nine participants, precluding robust analysis. These within-patient analyses were constrained by limited sample size (n = 25–36) and a restricted range of metabolic phenotypes within a single diagnostic category.

3.12. Sensitivity Analysis Restricted by Reported Fasting Duration

To assess whether the between-group differences depended on the imbalance in reported fasting duration, the eight principal features were re-analysed in the 45 participants reporting fasting >8 h but <10 h (13 patients and 32 controls). In this subset, all eight features differed in the same direction as in the full cohort, both without adjustment (all FDR ≤ 0.0012) and after adjustment for age, sex, and BMI (n = 44; all FDR ≤ 0.028) (Table 2; Table S5g). Adjusted effect estimates in the restricted subset were 0.75–1.28 times those in the full cohort, and the 95% confidence intervals overlapped for every feature. For example, TAG 54:6 was 2.36 log2 units lower (95% CI −2.82 to −1.90) and PI 36:1 was 0.93 log2 units lower (95% CI −1.25 to −0.61) in patients than in controls, compared with 2.17 (95% CI −2.61 to −1.72) and 0.93 (95% CI −1.15 to −0.72) log2 units lower in the full cohort. The largest attenuation was observed for PC 38:4 (0.22 vs. 0.29 log2 units higher; restricted 95% CI 0.03 to 0.42). Within the T2DM group, none of the eight features differed significantly between patients reporting fasting ≥10 h and those reporting >8 h but <10 h after adjustment for age, sex, and BMI (n = 30–32; all FDR ≥ 0.71), although the confidence intervals were wide (Table 2). AUCs in the restricted subset (0.808–0.983) were similar to those in the full cohort (0.795–0.985), with wider bootstrap confidence intervals (Table S5g). Because only 13 patients reported fasting <10 h, these analyses have limited precision and cannot exclude residual confounding by fasting duration or by other factors that differ between groups.

Table 2. Differences in the principal lipid features between participants with T2DM and controls in the full cohort and in participants reporting fasting >8 h but <10 h, and differences by reported fasting category within the T2DM group.

Lipid Species (Peak ID)	Full Cohort (n = 63–65)	Restricted to >8 h but <10 h (n = 44)	Within T2DM: ≥10 h vs. >8 h but <10 h (n = 30–32)
PI 36:1 (4157)	−0.93 (−1.15, −0.72)	−0.93 (−1.25, −0.61)	−0.04 (−0.32, 0.24)
PC 32:2 (2566)	−0.85 (−1.17, −0.54)	−1.09 (−1.52, −0.67)	0.31 (−0.16, 0.79)
TAG 54:6 (4284)	−2.17 (−2.61, −1.72)	−2.36 (−2.82, −1.90)	0.48 (−0.39, 1.34)
TAG 48:4 (3369)	−1.26 (−1.94, −0.58)	−1.25 (−2.17, −0.34)	−0.24 (−1.34, 0.86)
PC 40:8 (3521)	0.81 (0.57, 1.05)	0.74 (0.43, 1.04)	0.15 (−0.23, 0.53)
PE 38:1 (2860)	0.71 (0.46, 0.95)	0.74 (0.44, 1.04)	−0.14 (−0.53, 0.24)
PC 38:4 (3286)	0.29 (0.16, 0.43)	0.22 (0.03, 0.42)	0.09 (−0.08, 0.26)
PC 38:5 (3256)	0.49 (0.25, 0.73)	0.52 (0.18, 0.86)	0.09 (−0.25, 0.43)

Values are regression coefficients (95% CI) in log2 units from linear models adjusted for age, sex, and BMI: T2DM minus control (full cohort and restricted subset) and ≥10 h minus >8 h but <10 h (within T2DM). Full cohort, n = 65 (TAG 48:4, n = 63); restricted subset, 12 patients and 32 controls; within T2DM, n = 32 (TAG 48:4, n = 30). Benjamini–Hochberg FDR across the eight features: full cohort, all < 0.001; restricted subset, all ≤ 0.028; within T2DM, all ≥ 0.71. Unadjusted estimates, p-values, and AUCs are given in Table S5g.

4. Discussion

4.1. Principal Findings and Pathway-Level Interpretation

The present exploratory study suggests that untargeted serum lipidomic profiling can distinguish individuals with T2DM from control participants through coordinated alterations across multiple lipid species rather than through a single dominant biomarker. At the global level, the partial separation observed in the multivariate analyses indicates that T2DM is associated with a broad shift in the circulating lipidome, consistent with the systemic metabolic dysregulation linked to insulin resistance and impaired metabolic homeostasis [23]. The discriminatory pattern identified was driven predominantly by alterations in specific phospholipid and glycerolipid subclasses, most notably PC, PE, PI, and TAG. At the class level, total lipid abundance changed only modestly across groups, whereas stronger disease-related differences emerged at the level of individual molecular species, indicating that lipid remodeling in T2DM was selective rather than uniform across whole lipid classes. Among the most robust disease-associated signals, the polyunsaturated species PC 38:4, PC 38:5, and PC 40:8 and the species PE 38:1 were increased in T2DM, whereas PI 36:1, TAG 54:6, and PC 32:2 were consistently decreased. Within the PE subclass, PE 36:1 was elevated predominantly in female patients, and PE 34:1 showed a sex-associated pattern rather than a disease effect. This combination of increased polyunsaturated PC species, reduced PI, TAG, and less unsaturated PC species, and heterogeneous PE behavior suggests coordinated remodeling across interconnected phospholipid and glycerolipid pathways rather than isolated perturbation of a single lipid branch. In this context, diabetic dyslipidemia appears to involve selective changes in structurally and functionally distinct lipid molecular species that may reflect altered membrane composition, lipid signaling, and glycerolipid turnover. Some individual species, including PI 36:1 (AUC = 0.985), TAG 54:6 (AUC = 0.955), and PC 40:8 (AUC = 0.948), separated T2DM and control participants within this sample, and the separation persisted after adjustment for age, sex, and BMI, under cross-validation, and in participants with comparable reported fasting duration. However, these findings demonstrate an association with established T2DM rather than diagnostic utility, and because neither insulin resistance nor glycemic status was measured in controls, it remains unclear whether the identified species are specific to diabetes or reflect broader metabolic dysfunction, including obesity and insulin resistance. Accordingly, (Figure 10) is best interpreted as a conceptual pathway-level synthesis of the observed lipid alterations, placing the principal discriminatory species within an integrated network of phospholipid and glycerolipid metabolism. Importantly, this schematic should not be construed as direct evidence of metabolic flux, enzymatic activity, or causal directionality within pathways; rather, it is intended as a conceptual biological framework for contextualizing how the observed species-level alterations may relate to interconnected lipid metabolic processes in T2DM.

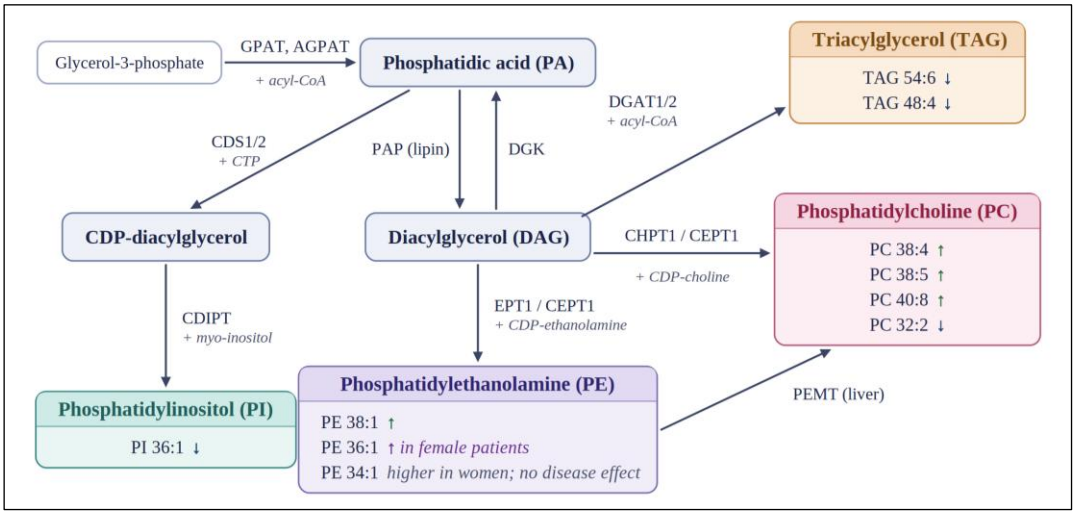


Figure 10. Simplified schematic of the glycerophospholipid and glycerolipid biosynthetic pathways linking the lipid classes discussed in this study. Glycerol-3-phosphate is acylated to phosphatidic acid (PA) by glycerol-3-phosphate acyltransferases and acylglycerol-3-phosphate acyltransferases (GPAT, AGPAT). PA is converted by phosphatidic acid phosphatase (PAP; lipin) to diacylglycerol (DAG), which diacylglycerol kinase (DGK) can recycle to PA, or by CDP-diacylglycerol synthases (CDS1/2) to CDP-diacylglycerol, from which CDP-diacylglycerol–inositol 3-phosphatidyltransferase (CDIPT) forms phosphatidylinositol (PI). DAG is the acceptor of the CDP-choline and CDP-ethanolamine pathways, in which choline/ethanolamine phosphotransferases (CHPT1, CEPT1, and EPT1) form phosphatidylcholine (PC) and phosphatidylethanolamine (PE) and is acylated to triacylglycerol (TAG) by diacylglycerol O-acyltransferases (DGAT1/2). In the liver, PE can be methylated to PC by phosphatidylethanolamine N-methyltransferase (PEMT). Co-substrates are shown in italics.

4.2. Altered Phospholipid and Glycerolipid Metabolism in T2DM

The biochemical basis for the observed lipidomic segregation may reside in perturbations of core pathways regulating phospholipid and glycerolipid homeostasis. Phospholipid and glycerolipid biosynthesis is organized around shared metabolic intermediates, particularly diacylglycerol and cytidine diphosphate-diacylglycerol, which act as major branch points linking the biosynthetic routes of PC, PE, PI, and TAG [24]. Accordingly, disturbance of these interconnected nodes could produce coordinated but non-uniform changes across several lipid classes, as observed in the present dataset. Within this framework, the concurrent increase in several polyunsaturated PC species and PE 38:1, together with the decrease in PI 36:1, TAG 54:6, and PC 32:2, is consistent with broader remodeling of phospholipid and glycerolipid metabolism in T2DM rather than isolated dysregulation of a single lipid class. This interpretation is further supported by the finding that class-level lipid abundance changed only modestly across groups, whereas clearer differences emerged at the level of individual molecular species. Previous studies have shown that the balance between membrane phospholipid synthesis and neutral lipid storage is tightly regulated and may be altered under conditions of insulin resistance and hepatic metabolic stress [25,26]. In that context, the pattern observed here may reflect redistribution within interconnected lipid metabolic pathways, potentially affecting membrane composition, lipid signaling, and glycerolipid turnover.

4.3. Phosphatidylcholine and Phosphatidylethanolamine Remodeling

Among the lipid classes evaluated, the most consistent disease-associated pattern was observed at the level of selected phosphatidylcholine molecular species rather than total class abundance. PC 38:4, PC 38:5, and PC 40:8 were increased in participants with

T2DM relative to controls, with female patients generally showing the highest signal intensities, whereas PC 32:2 was decreased. The PC changes were therefore not uniform: the increased species contain more acyl carbons and double bonds (four to eight), whereas the decreased species contains only two, suggesting a shift in the acyl-chain composition of circulating PC rather than a change in total PC; species-specific PC alterations in T2DM have also been reported in a recent untargeted and targeted lipidomic study [20]. Alterations in the phospholipid species composition of skeletal muscle have previously been associated with metabolic syndrome in humans and with insulin resistance in a rat model of prediabetes, in both cases involving decreases in specific phospholipids [27,28]. Moreover, a potentially relevant aspect of these findings is the metabolic interrelationship between PC and PE; the conversion of PE to PC via phosphatidylethanolamine N-methyltransferase represents a central node in phospholipid homeostasis and has been increasingly implicated in hepatic lipid handling and systemic insulin sensitivity [29,30]. An elevated PC/PE ratio has been proposed as an index of metabolic dysfunction and insulin resistance across multiple tissues, including skeletal muscle [27,28]. In the present dataset, however, PC and PE species did not change in opposite directions (PE 38:1 and PE 36:1 were increased, as were several PC species), and the PC/PE ratio, enzyme activity, and pathway flux were not quantified; we therefore do not interpret these findings as evidence of altered PEMT activity. PE species showed a heterogeneous profile, PE 38:1 was increased in both sexes, PE 36:1 was increased predominantly in female patients, and PE 34:1 showed a sex-associated pattern without a disease effect. Together, these observations suggest that phospholipid alterations in T2DM are species-specific and modulated by both disease-related processes and sex. Furthermore, because the annotations are at the sum-composition level, each species may comprise several molecular species; this is illustrated by a second PC 40:8 feature (Peak ID 3520) that was lower rather than higher in T2DM. We therefore refrain from attributing specific physiological functions to these incompletely characterized species.

4.4. PI and TAG Remodeling in T2DM

The observed decrease in PI 36:1 in participants with T2DM is of potential biological interest given the broader role of phosphatidylinositol-containing lipids in membrane-associated signaling and metabolic regulation [31,32]. In the present dataset, PI 36:1 showed a clear and consistent reduction in both diabetic subgroups relative to controls, with strong statistical support after multiple-testing correction. Because total PI abundance changed only modestly at the class level, this finding is best interpreted as a species-specific alteration rather than a generalized reduction of the entire PI subclass. A similarly important observation was the reduction in selected TAG species, particularly TAG 54:6, which showed the strongest disease-associated decrease, whereas TAG 48:4 showed a weaker but still significant reduction, and TAG 52:4 and TAG 54:4 did not remain significant after multiple-testing correction. This pattern indicates that TAG remodeling in T2DM was selective and species-specific rather than uniformly increased or decreased across the whole TAG class. At first glance, the reduction in TAG 54:6 may appear paradoxical because T2DM is commonly associated with hypertriglyceridemia in routine clinical testing [33]. However, the present result concerns individual TAG molecular species rather than total circulating triglycerides, and the class-level boxplots showed only modest overall differences in summed TAG abundance across the four subgroups. Accordingly, the present findings support the view that glycerolipid dysregulation in T2DM involves selective remodeling of individual TAG species rather than a uniform shift in all TAG molecules [34,35]. Consistent with this, TAG 54:6 was not correlated with conventional serum triglycerides among patients (ϱ = 0.22), and its reduction persisted after adjustment for age, sex, and BMI. The direction of this finding is

in line with the observation from the Rhee et al. [36] that TAG species with higher acyl carbon number and double-bond content were associated with lower risk of T2DM, whereas species with lower carbon number and double-bond content were associated with higher risk and with insulin resistance. Nevertheless, TAG 54:6 may represent several molecular species with different fatty acyl combinations (such as, 18:2/18:2/18:2, 18:1/18:2/18:3, or 16:0/18:2/20:4), whose abundance is strongly influenced by dietary fatty acid intake; dietary modification after diagnosis, lipid-lowering and glucose-lowering treatment, and the higher variability of this feature in patients may therefore contribute. With respect to lipotoxicity, lipid classes are most directly implicated in lipotoxic insulin resistance, such as diacylglycerols and ceramides [12]. The features identified here therefore cannot currently serve as surrogate markers of lipotoxicity; whether the observed shifts in TAG and phospholipid species relate to lipotoxic burden or cardiovascular risk in T2DM should be examined in studies that measure these lipid mediators together with cardiovascular outcomes.

4.5. Sex-Associated Subgroup Patterns and Biomarker Implications

A further important aspect of the present study was the presence of subgroup patterns suggestive of sex-related variation in selected lipid species. PE 34:1 showed the clearest sex-associated subgroup pattern, with higher levels in the female subgroups overall, whereas PE 36:1 was increased predominantly in female patients with T2DM, the only species for which a sex-by-disease interaction was statistically supported; by contrast, PE 38:1 showed a disease-associated increase in both sexes. These findings suggest that lipid remodeling in T2DM is influenced not only by disease status but also by subgroup-dependent biological variation [37]. For that reason, future lipidomic studies in T2DM should incorporate sex explicitly as a biological variable in both study design and downstream analysis; from a translational perspective, the present data also indicate that lipid-based discrimination of T2DM is more likely to rely on multi-lipid signatures than on a single molecule. The top discriminatory panel showed a bidirectional pattern in which reduced PI, PC 32:2, and TAG signals coexisted with increased polyunsaturated PC species and PE 38:1. In the ROC analysis, PI 36:1, TAG 54:6, and PC 40:8 showed the highest AUCs (0.985, 0.955, and 0.948, respectively), and cross-validation in which feature selection was repeated within each training fold yielded a similar estimate for the top-ranked feature (0.954).

4.6. Limitations and Future Directions

A key strength of this study is the application of untargeted UPLC-MS-based lipidomics to characterize serum lipid perturbations in individuals with T2DM and control participants. This approach captured both broad lipid-class patterns and alterations in individual putatively annotated species across phosphatidylcholine, phosphatidylethanolamine, phosphatidylinositol, and triacylglycerol subclasses. The integration of multivariate profiling with feature-level analyses further enabled the identification of candidate discriminatory lipid features. Nevertheless, some limitations should be considered when interpreting the findings. First, the sample size was modest, which may have limited statistical power and the external validity of the identified lipid signatures, particularly in sex-stratified analyses. The sex distribution was also unequal, especially among male participants. Accordingly, the sex-specific findings should be regarded as exploratory and hypothesis-generating rather than confirmatory. Second, the cross-sectional design precludes causal inference. The observed lipid alterations should therefore be interpreted as disease-associated correlates within this cohort and not as causal determinants of T2DM. Third, lipidomic measurements were performed in serum rather than plasma; serum lipid abundances may be influenced by coagulation-related

and other pre-analytical processes, which may be particularly relevant for phospholipid species. In addition, the blood collection tubes were not cooled immediately after venipuncture but were allowed to clot at ambient temperature according to the serum-processing protocol. Although this procedure was applied consistently to all participants, it may have affected the concentrations of some lipid species. The present findings should therefore be interpreted as serum-specific and require validation in plasma-based studies. Fourth, residual confounding cannot be excluded; although the principal associations persisted after adjustment for age, sex, and BMI, disease status was inherently linked to treatment exposure: participants with T2DM, but not the control participants, had diagnosed diabetes, and some participants with T2DM were receiving glucose-lowering and/or lipid-lowering therapy. Consequently, the independent contributions of diabetes and treatment cannot be fully separated in this dataset. Dietary intake, physical activity, and diabetes duration were incompletely recorded and could not be incorporated into the models. Fifth, the coefficient of variation estimates were calculated across biological samples rather than from replicate pooled quality-control measurements; they therefore describe combined biological-sample variability and analytical variation, rather than analytical precision alone. Two reported TAG features, TAG 54:6 and TAG 48:4, exceeded the prespecified median-CV flag of 50%. These findings should be considered when interpreting the reliability and reproducibility of the corresponding feature-level associations. Sixth, the ROC estimates were obtained in a single case–control sample of participants with established T2DM and control participants and were internally cross-validated only; no independent replication cohort was available. The near-complete separation achieved by some multi-lipid models may therefore overestimate performance in clinically relevant populations. In addition, systematic pre-analytical differences between groups, including possible differences in collection period or storage duration, could have contributed to the observed separation. Because replicate pooled-QC data were not available for estimating feature-specific analytical precision, the extent of this contribution cannot be quantified from the present dataset. Seventh, reported fasting duration was imbalanced between the study groups: all participants reported an overnight fast of more than 8 h, but 23/36 participants with T2DM and 1/33 control participants reported fasting for at least 10 h. Fasting duration was self-reported, recorded only as a binary category, and not independently verified. In a sensitivity analysis restricted to participants reporting fasting >8 h but <10 h, all eight principal associations persisted with similar effect estimates and AUCs, and fasting category was not significantly associated with lipid levels within the T2DM group. These results suggest that the principal between-group differences are not explained by the fasting imbalance alone. However, the restricted analysis included only 13 patients (12 with complete covariate data), the binary categories cannot capture variation in fasting duration within each category, and residual confounding by fasting duration or other pre-analytical conditions cannot be excluded. The ROC estimates should therefore still be interpreted as exploratory and cohort-specific rather than as evidence of diagnostic performance. The plasma glucose and triglyceride measurements used to calculate the TyG index were obtained from the same blood collection as the lipidomic measurements; however, the index should not be interpreted as having been uniformly derived after a confirmed 10-h fast. Eighth, the reported lipid species assignments are putative and require confirmation by targeted tandem mass spectrometry and comparison with authentic reference standards. In addition, isotope-labelled or class-specific internal standards were not incorporated into the untargeted workflow. This may limit the accuracy and comparability of quantitative estimates across lipid classes. Therefore, despite the use of pooled quality-control samples and solvent blanks, the findings should be interpreted primarily as relative differences in feature abundance rather than as fully validated

absolute concentrations. Future studies should validate these candidate lipid biomarkers in larger, independent cohorts under balanced and prospectively standardized fasting conditions. Longitudinal sampling coupled with more comprehensive clinical phenotyping would facilitate discrimination of disease-associated alterations from treatment-related effects and temporal variability. Targeted quantitative lipidomics will be essential to confirm both the magnitude and directionality of the observed changes, whereas integrative analyses incorporating transcriptomic, proteomic, and enzyme-activity data may elucidate the biological pathways underlying the dysregulated phospholipid and glycerolipid signatures. In addition, it will be important to assess whether the identified lipid features are associated with insulin resistance, glycaemic control, hepatic steatosis, and diabetes-related complications.

5. Conclusions

In this exploratory case–control study, established T2DM was associated with a distinct serum lipidomic profile involving selected phospholipid and glycerolipid species rather than isolated perturbations in single lipid species. Specifically, patients showed higher levels of several polyunsaturated phosphatidylcholine species and lower levels of PC 32:2, heterogeneous and species-specific differences in phosphatidylethanolamines, and lower levels of phosphatidylinositol 36:1 and triacylglyceride 54:6; these associations persisted after adjustment for age, sex, and BMI and in participants with comparable reported fasting duration. These observations are consistent with a selective alteration of lipid homeostasis involving both membrane-associated and storage lipids, but the cross-sectional design, the putative sum-composition annotations, and the absence of laboratory phenotyping in controls do not allow mechanistic conclusions or a distinction between diabetes-specific changes and broader metabolic dysfunction. The high discriminatory performance observed within this sample should not be interpreted as diagnostic utility. Validation in larger, independent cohorts that include individuals across the spectrum of glycemia and insulin resistance, using plasma-based and targeted quantitative lipidomics with structural confirmation, will be essential to determine whether the observed lipid alterations are robust and clinically informative.

Supplementary Materials: The following supporting information can be downloaded at: https://www.mdpi.com/article/10.3390/biomedicines14112472/s1, Table S1. Comprehensive demographic characteristics of control subjects and individuals diagnosed with T2DM. Table S2. Coefficient of variation (CV%) values for each of the 92 annotated lipid features. Table S3. Raw lipidomic data as indicated by peak ID for control individuals and T2DM patients. Table S4. Normalized intensities of the 92 putatively annotated lipid features as indicated by peak ID for control individuals and T2DM patients. Table S5. Statistics for all 92 annotated features (S5a), age-, sex- and BMI-adjusted models and sex-by-disease interaction (S5b), correlations with clinical parameters within the T2DM group (S5c), medication comparisons (S5d), bootstrap confidence intervals of AUCs (S5e), internal validation (S5f), and fasting-restricted sensitivity analyses (S5g). Figure S1. Demographic characteristics of the study cohort: (a) Heatmap showing the distribution of self-reported nationality across FC, MC, FP, and MP. (b) Violin plots showing the age distribution across the four study subgroups.

Author Contributions: J.Y.A.-A., H.B.A.M., A.A.E., A.F.B., O.H.E. and S.E. contributed to the conception and design of the study. J.Y.A.-A., H.B.A.M., R.Z., K.B., A.A., H.H.M., S.B., and A.S.A. contributed to participant recruitment, clinical assessment, and sample collection. R.Z., A.B., LW, A.A.E., O.H.E., A.F.B. and S.E. contributed to the experimental work and lipidomic analyses. J.Y.A.-A., H.B.A.M., R.Z., A.B., L.W., A.A.E., O.H.E., and S.E. contributed to data analysis and interpretation. J.Y.A.-A. and S.E. drafted the manuscript. H.B.A.M., K.B., A.A., H.H.M., S.B., A.B.,

L.W., A.S.A., A.A.E., and O.H.E. critically revised the manuscript for important intellectual content. All authors have read and agreed to the published version of the manuscript.

Funding: This project was funded by the Deanship of Scientific Research (DSR) at King Abdulaziz University, Jeddah, under grant no. (3-6-1432/HiCi). The Authors, therefore, acknowledge with thanks DSR for technical and financial support.

Institutional Review Board Statement: The study was conducted in accordance with the Declaration of Helsinki and approved by the Institutional Review Board (Unit of Biomedical Ethics, Faculty of Medicine, King Abdulaziz University) (protocol code IEE-20; date of approval: 1 October 2018).

Informed Consent Statement: Informed consent was obtained from all subjects involved in the study.

Data Availability Statement: The data supporting the findings of this study are provided in the Supplementary Materials (Tables S1–S5).

Acknowledgments: The authors thank all participants who took part in this study. Further thanks go to the Deanship of Scientific Research (DSR) at King Abdulaziz University, Jeddah, for support under grant no. (3-6-1432/HiCi).

Conflicts of Interest: The authors declare no conflicts of interest.

Abbreviations

The following abbreviations are used in this manuscript:

T2DM	Type 2 diabetes mellitus
UPLC-MS	Ultra-performance liquid chromatography-mass spectrometry
PE	Phosphatidylethanolamine
PC	Phosphatidylcholine
PI	Phosphatidylinositol
TAG	Triacylglyceride
HbA1c	Glycated hemoglobin
BMI	Body mass index
ADA	American Diabetes Association
FDR	False discovery rate
FC	Female control
MC	Male control
FP	Female patient
MP	Male patient
AUC	Area under the curve
CV	Coefficient of variation
HCA	Hierarchical clustering analysis
non-HDL-C	Non-high-density lipoprotein cholesterol
PCA	Principal component analysis
QC	Quality control
ROC	Receiver operating characteristic
TyG	Triglyceride-glucose index

References

1. Rob, A.; Hoque, A.; Asaduzzaman, M.M.; Khatoon, M.A.A.; Khalil, R.; Thomas, D.; Ilyas, M.; Mahmood, H.; Chowdhury, T.A. The Global Challenges of Type 2 Diabetes. *Bangladesh J. Med.* **2025**, *36*, 92–98. https://doi.org/10.3329/bjm.v36i2.78406.
2. Kane, J.P.; Pullinger, C.R.; Goldfine, I.D.; Malloy, M.J. Dyslipidemia and diabetes mellitus: Role of lipoprotein species and interrelated pathways of lipid metabolism in diabetes mellitus. *Curr. Opin. Pharmacol.* **2021**, *61*, 21–27. https://doi.org/10.1016/j.coph.2021.08.013.

3. DeFronzo, R.A.; Tripathy, D. Skeletal muscle insulin resistance is the primary defect in type 2 diabetes. *Diabetes Care* **2009**, *32*, S157–S163. https://doi.org/10.2337/dc09-S302.
4. Bays, H.E.; Gonzalez-Campoy, J.M.; Bray, G.A.; Kitabchi, A.E.; Bergman, D.A.; Schorr, A.B.; Rodbard, H.W.; Henry, R.R. Pathogenic potential of adipose tissue and metabolic consequences of adipocyte hypertrophy and increased visceral adiposity. *Expert. Rev. Cardiovasc. Ther.* **2008**, *6*, 343–368. https://doi.org/10.1586/14779072.6.3.343.
5. Zhao, X.; An, X.; Yang, C.; Sun, W.; Ji, H.; Lian, F. The crucial role and mechanism of insulin resistance in metabolic disease. *Front. Endocrinol.* **2023**, *14*, 1149239. https://doi.org/10.3389/fendo.2023.1149239.
6. Zhong, X.; Xiao, C.; Wang, R.; Deng, Y.; Du, T.; Li, W.; Zhong, Y.; Tan, Y. Lipidomics based on UHPLC/Q-TOF-MS to characterize lipid metabolic profiling in patients with newly diagnosed type 2 diabetes mellitus with dyslipidemia. *Heliyon* **2024**, *10*, e26326. https://doi.org/10.1016/j.heliyon.2024.e26326.
7. Xuan, Q.; Hu, C.; Zhang, Y.; Wang, Q.; Zhao, X.; Liu, X.; Wang, C.; Jia, W.; Xu, G. Serum lipidomics profiles reveal potential lipid markers for prediabetes and type 2 diabetes in patients from multiple communities. *Front. Endocrinol.* **2022**, *13*, 966823. https://doi.org/10.3389/fendo.2022.966823.
8. Lopez-Lopez, A.; Lopez-Gonzalvez, A.; Barbas, C. Metabolomics for searching validated biomarkers in cancer studies: A decade in review. *Expert Rev. Mol. Diagn.* **2024**, *24*, 601–626. https://doi.org/10.1080/14737159.2024.2368603.
9. Hannun, Y.A.; Obeid, L.M. Principles of bioactive lipid signalling: Lessons from sphingolipids. *Nat. Rev. Mol. Cell Biol.* **2008**, *9*, 139–150. https://doi.org/10.1038/nrm2329.
10. Jahdkaran, M.; Sistanizad, M. From lipids to glucose: Investigating the role of dyslipidemia in the risk of insulin resistance. *J. Steroid Biochem. Mol. Biol.* **2025**, *250*, 106744. Erratum in *J Steroid Biochem Mol Biol*. **2026**, *255*, 106876. https://doi.org/10.1016/j.jsbmb.2025.106744.
11. Tracey, T.J.; Steyn, F.J.; Wolvetang, E.J.; Ngo, S.T. Neuronal Lipid Metabolism: Multiple Pathways Driving Functional Outcomes in Health and Disease. *Front. Mol. Neurosci.* **2018**, *11*, 10. https://doi.org/10.3389/fnmol.2018.00010.
12. Petersen, M.C.; Shulman, G.I. Roles of Diacylglycerols and Ceramides in Hepatic Insulin Resistance. *Trends Pharmacol. Sci.* **2017**, *38*, 649–665. https://doi.org/10.1016/j.tips.2017.04.004.
13. Ruze, R.; Liu, T.; Zou, X.; Song, J.; Chen, Y.; Xu, R.; Yin, X.; Xu, Q. Obesity and type 2 diabetes mellitus: Connections in epidemiology, pathogenesis, and treatments. *Front. Endocrinol.* **2023**, *14*, 1161521. https://doi.org/10.3389/fendo.2023.1161521.
14. Hameed, A.; Mojsak, P.; Buczynska, A.; Suleria, H.A.R.; Kretowski, A.; Ciborowski, M. Altered Metabolome of Lipids and Amino Acids Species: A Source of Early Signature Biomarkers of T2DM. *J. Clin. Med.* **2020**, *9*, *2257*. https://doi.org/10.3390/jcm9072257.
15. Karagiannidis, E.; Moysidis, D.V.; Papazoglou, A.S.; Panteris, E.; Deda, O.; Stalikas, N.; Sofidis, G.; Kartas, A.; Bekiaridou, A.; Giannakoulas, G.; et al. Prognostic significance of metabolomic biomarkers in patients with diabetes mellitus and coronary artery disease. *Cardiovasc. Diabetol.* **2022**, *21*, 70. https://doi.org/10.1186/s12933-022-01494-9.
16. Anh, N.K.; Thu, N.Q.; Tien, N.T.N.; Long, N.P.; Nguyen, H.T. Advancements in Mass Spectrometry-Based Targeted Metabolomics and Lipidomics: Implications for Clinical Research. *Molecules* **2024**, *29*, 5934. https://doi.org/10.3390/molecules29245934.
17. Xu, T.; Hu, C.; Xuan, Q.; Xu, G. Recent advances in analytical strategies for mass spectrometry-based lipidomics. *Anal. Chim. Acta* **2020**, *1137*, 156–169. https://doi.org/10.1016/j.aca.2020.09.060.
18. Latha, V.A.; Mondu, S.S.D.; Dinesh Eshwar, M.; Polala, A.R.; Nandanavanam, S.; Dodda, S. Dyslipidemia Among Diabetes Mellitus Patients: A Case-Control Study From a Tertiary Care Hospital in South India. *Cureus* **2023**, *15*, e35625. https://doi.org/10.7759/cureus.35625.
19. American Diabetes Association Professional Practice, C. 2. Diagnosis and Classification of Diabetes: Standards of Care in Diabetes-2024. *Diabetes Care* **2024**, *47*, S20–S42. https://doi.org/10.2337/dc24-S002.
20. Feng, L.; He, B.; Xia, J.; Wang, Z. Untargeted and Targeted Lipidomics Unveil Dynamic Lipid Metabolism Alterations in Type 2 Diabetes. *Metabolites* **2024**, *14*, 610. https://doi.org/10.3390/metabo14110610.
21. Liebisch, G.; Fahy, E.; Aoki, J.; Dennis, E.A.; Durand, T.; Ejsing, C.S.; Fedorova, M.; Feussner, I.; Griffiths, W.J.; Köfeler, H.; et al. Update on LIPID MAPS classification, nomenclature, and shorthand notation for MS-derived lipid structures. *J. Lipid Res.* **2020**, *61*, 1539–1555. https://doi.org/10.1194/jlr.S120001025.
22. Simental-Mendia, L.E.; Rodriguez-Moran, M.; Guerrero-Romero, F. The product of fasting glucose and triglycerides as surrogate for identifying insulin resistance in apparently healthy subjects. *Metab. Syndr. Relat. Disord.* **2008**, *6*, 299–304. https://doi.org/10.1089/met.2008.0034.

23. Chew, W.S.; Torta, F.; Ji, S.; Choi, H.; Begum, H.; Sim, X.; Khoo, C.M.; Khoo, E.Y.H.; Ong, W.Y.; Van Dam, R.M.; et al. Large-scale lipidomics identifies associations between plasma sphingolipids and T2DM incidence. *JCI Insight* **2019**, *5*, e126925. https://doi.org/10.1172/jci.insight.126925.
24. Blunsom, N.J.; Cockcroft, S. CDP-Diacylglycerol Synthases (CDS): Gateway to Phosphatidylinositol and Cardiolipin Synthesis. *Front. Cell Dev. Biol.* **2020**, *8*, 63. https://doi.org/10.3389/fcell.2020.00063.
25. Perez-Marti, A.; Ramakrishnan, S.; Li, J.; Dugourd, A.; Molenaar, M.R.; De La Motte, L.R.; Grand, K.; Mansouri, A.; Parisot, M.; Lienkamp, S.S.; et al. Reducing lipid bilayer stress by monounsaturated fatty acids protects renal proximal tubules in diabetes. *Elife* **2022**, *11*, e74391. https://doi.org/10.7554/eLife.74391.
26. Desai, A.J.; Miller, L.J. Changes in the plasma membrane in metabolic disease: Impact of the membrane environment on G protein-coupled receptor structure and function. *Br. J. Pharmacol.* **2018**, *175*, 4009–4025. https://doi.org/10.1111/bph.13943.
27. Adamson, S.E.; Adak, S.; Petersen, M.C.; Higgins, D.; Spears, L.D.; Zhang, R.M.; Cedeno, A.; McKee, A.; Kumar, A.; Singh, S.; et al. Decreased sarcoplasmic reticulum phospholipids in human skeletal muscle are associated with metabolic syndrome. *J. Lipid Res.* **2024**, *65*, 100519. https://doi.org/10.1016/j.jlr.2024.100519.
28. Markova, I.; Huttl, M.; Stastny, J.; Zapletalova, I.; Kacer, P.; Honig, V.; Kacerova, T.; Malinska, H. Skeletal muscle insulin resistance in prediabetes: A lipidomic perspective on diacylglycerols, ceramides, and phospholipids. *Sci. Rep.* **2025**, *15*, 38784. https://doi.org/10.1038/s41598-025-22745-1.
29. van der Veen, J.N.; Kennelly, J.P.; Wan, S.; Vance, J.E.; Vance, D.E.; Jacobs, R.L. The critical role of phosphatidylcholine and phosphatidylethanolamine metabolism in health and disease. *Biochim. Biophys. Acta Biomembr.* **2017**, *1859*, 1558–1572. https://doi.org/10.1016/j.bbamem.2017.04.006.
30. Li, J.; Xin, Y.; Li, J.; Chen, H.; Li, H. Phosphatidylethanolamine N-methyltransferase: From Functions to Diseases. *Aging Dis.* **2023**, *14*, 879–891. https://doi.org/10.14336/AD.2022.1025.
31. Katan, M.; Cockcroft, S. Phosphatidylinositol(4,5)bisphosphate: Diverse functions at the plasma membrane. *Essays Biochem.* **2020**, *64*, 513–531. https://doi.org/10.1042/EBC20200041.
32. Cao, R.; Tian, H.; Zhang, Y.; Liu, G.; Xu, H.; Rao, G.; Tian, Y.; Fu, X. Signaling pathways and intervention for therapy of type 2 diabetes mellitus. *MedComm (2020)* **2023**, *4*, e283. https://doi.org/10.1002/mco2.283.
33. Dharmalingam, M.; Yamasandhi, P.G. Nonalcoholic Fatty Liver Disease and Type 2 Diabetes Mellitus. *Indian. J. Endocrinol. Metab.* **2018**, *22*, 421–428. https://doi.org/10.4103/ijem.IJEM_585_17.
34. Qiu, G.; Wang, H.; Yan, Q.; Ma, H.; Niu, R.; Lei, Y.; Xiao, Y.; Zhou, L.; Yang, H.; Xu, C.; et al. A Lipid Signature with Perturbed Triacylglycerol Co-Regulation, Identified from Targeted Lipidomics, Predicts Risk for Type 2 Diabetes and Mediates the Risk from Adiposity in Two Prospective Cohorts of Chinese Adults. *Clin. Chem.* **2022**, *68*, 1094–1107. https://doi.org/10.1093/clinchem/hvac090.
35. Zhang, S.; Jiang, X.; Zhang, S.; Zong, Y.; Zheng, S.; Feng, Q.; Gao, Y.; Zheng, J. Lipidomic signatures in gestational diabetes mellitus and postpartum type 2 diabetes mellitus: A narrative review of etiologic and predictive implications. *EBioMedicine* **2026**, *129*, 106349. https://doi.org/10.1016/j.ebiom.2026.106349.
36. Rhee, E.P.; Cheng, S.; Larson, M.G.; Walford, G.A.; Lewis, G.D.; McCabe, E.; Yang, E.; Farrell, L.; Fox, C.S.; O'Donnell, C.J.; et al. Lipid profiling identifies a triacylglycerol signature of insulin resistance and improves diabetes prediction in humans. *J. Clin. Investig.* **2011**, *121*, 1402–1411. https://doi.org/10.1172/JCI44442.
37. Sanches, J.M.; Zhao, L.N.; Salehi, A.; Wollheim, C.B.; Kaldis, P. Pathophysiology of type 2 diabetes and the impact of altered metabolic interorgan crosstalk. *FEBS J.* **2023**, *290*, 620–648. https://doi.org/10.1111/febs.16306.

Disclaimer/Publisher's Note: The statements, opinions and data contained in all publications are solely those of the individual author(s) and contributor(s) and not of MDPI and/or the editor(s). MDPI and/or the editor(s) disclaim responsibility for any injury to people or property resulting from any ideas, methods, instructions or products referred to in the content.